

## 1. EARLY MIocene TO PLEISTOCENE DIATOM STRATIGRAPHY OF LEG 145<sup>1</sup>

John A. Barron<sup>2</sup> and Andrey Y. Gladenkov<sup>3</sup>

### ABSTRACT

Early Miocene through Pleistocene diatom datum levels are identified along with North Pacific diatom zones in the sections cored during Ocean Drilling Program Leg 145 at Sites 881 to 884 and 887. Recording of the first complete late early Miocene through Miocene magnetostratigraphies in the North Pacific at Sites 884 and 887 has allowed the first magnetostratigraphic calibration of over 40 diatom datum levels between Subchron C5En (18.817–18.317 Ma) and Subchron C3Bn (6.901–6.744 Ma). Absolute age estimates from these calibrations as well as from 20 younger (latest Miocene and Pliocene) magnetostratigraphic calibrations of diatom datum levels at Sites 881–884 and 887 are presented and compared with the published age estimates from the literature. Most of the late early Miocene through Pliocene diatom datum levels that have been widely used in the North Pacific for biostratigraphy appear to be roughly isochronous within the level of resolution constrained by sample spacing. Diachroneity across latitude, however, is revealed for a number of diatom events, including the first occurrences of *Actinocyclus ingens* var. *nodus*, *Simonsenella barboi*, and *Neodenticula koizumii*.

*Thalassiosira minutissima* Oreshkina, nov. sp., is described.

### INTRODUCTION

Over the past 20 yr, Miocene to Pleistocene North Pacific diatom stratigraphy has developed rapidly from the pioneering papers of Schrader (1973) and Koizumi (1973) through later papers by Koizumi (1975, 1980, 1985, 1992), Burckle and Opdyke (1977), Koizumi and Tanimura (1985), Barron (1980a, 1981, 1985b, 1992), Oreshkina (1985), Akiba (1986), and Akiba and Yanagisawa (1986). Akiba's (1986) paper is perhaps the best summary of the state of Miocene to Pleistocene North Pacific diatom stratigraphy, and his proposed stratigraphic zonation has been widely accepted. In spite of these excellent studies, there has been a lack of pre-latest Miocene (>6.0 Ma) calibration of diatom stratigraphy to magnetostratigraphy in the North Pacific (Koizumi and Tanimura, 1985; Barron, 1992).

Consequently, the recording of temporally lengthy Miocene magnetostratigraphic records at Sites 884 and 887 (Fig. 1) in the northwest and northeast Pacific during Ocean Drilling Program (ODP) Leg 145 (Rea, Basov, Janecek, Palmer-Julson, et al., 1993) represented a unique opportunity to refine the absolute age estimates of Miocene and Pliocene diatom levels in the North Pacific.

Leg 145 cored 25 holes at 7 sites in a west-to-east transect of the subarctic North Pacific (Fig. 1). Three of these sites (882, 883, and 887) were cored on top of seamounts, where carbonate-bearing sediments relatively free of terrigenous debris offered the best possibility of high-resolution paleoceanographic studies. Site 884, on the east flank of the Detroit Seamount, was cored to obtain a comparative record of deep-sea sedimentation and to record the history of the Meiji sediment tongue. Site 881 was selected to be a northern extension of the south-to-north paleoceanographic transect begun off Japan on Deep Sea Drilling Project (DSDP) Leg 86, whereas Sites 885 and 886 were located in the low biologic productivity region of the central North Pacific where a good record of eolian deposition was expected (Rea, Basov, Janecek, Palmer-Julson, et al., 1993).

Extensive Miocene to Pleistocene diatom records were recovered at each site. The purpose of this paper is to document the diatom stratigraphy at Sites 881 to 884 and 887 and to refine the calibration of diatom datum levels to the magnetostratigraphy. Because the paleomagnetic calibration of latest Pliocene and Pleistocene diatom datum levels in the North Pacific is relatively well known (Koizumi and Tanimura, 1985), the emphasis is placed on the refinement of diatom datum levels in Miocene and Pliocene sediments.

### METHODS

On board the *JOIDES Resolution*, strewn slides were prepared by placing a small amount of material in a snap-cap vial, adding distilled water, agitating the vial, and removing part of the upper suspension with a pipette. When required (because of a low concentration of diatoms or an induration of the sediment), selected samples were processed by boiling them in hydrogen peroxide and hydrochloric acid, and then using the centrifuge (at 1200 rpm for 2–4 min) to remove these chemicals from the suspension. In the laboratory, beakers were used in place of snap-cap vials. Acid-treated material was made pH-neutral by repeatedly filling and decanting the beakers with distilled water and allowing 4 hr or more for settling. Strewn slides were examined in their entirety at 500× for stratigraphic markers and other common taxa; generally, at least 1000 specimens were examined per slide. Identifications were checked routinely at 1250×.

The following references were used in selecting diatom datum levels for investigation: Koizumi (1985, 1992), Akiba (1986), Barron (1992), and Akiba et al. (1993). Because the stratigraphic distribution of diatoms in the North Pacific in the middle Miocene through Pleistocene is relatively well known from these studies, no attempt was made to provide distribution charts in sediments of these ages. For older sediments, however, a companion paper (Gladenkova and Barron, this volume) documents the distribution of diatom taxa in the Oligocene through lower Miocene of Site 884. No new diatom stratigraphic studies beyond those published in Rea, Basov, Janecek, Palmer-Julson, et al. (1993) were completed on the very thin (<50 m) biosiliceous sections cored at Sites 885 and 886, so they are not discussed in this paper.

### Taxonomy

The taxonomy used follows that of Koizumi (1980, 1992), Akiba (1986), Yanagisawa and Akiba (1990), Fenner (1991), Harwood and

<sup>1</sup> Rea, D.K., Basov, I.A., Scholl, D.W., and Allan, J.F. (Eds.), 1995. Proc. ODP, Sci. Results, 145: College Station, TX (Ocean Drilling Program).

<sup>2</sup> U.S. Geological Survey (MS 915), 345 Middlefield Road, Menlo Park, CA 94025, U.S.A.

<sup>3</sup> Institute of the Lithosphere, Russian Academy of Sciences, Staromonetny Per. 22, Moscow 109180, Russian Federation.

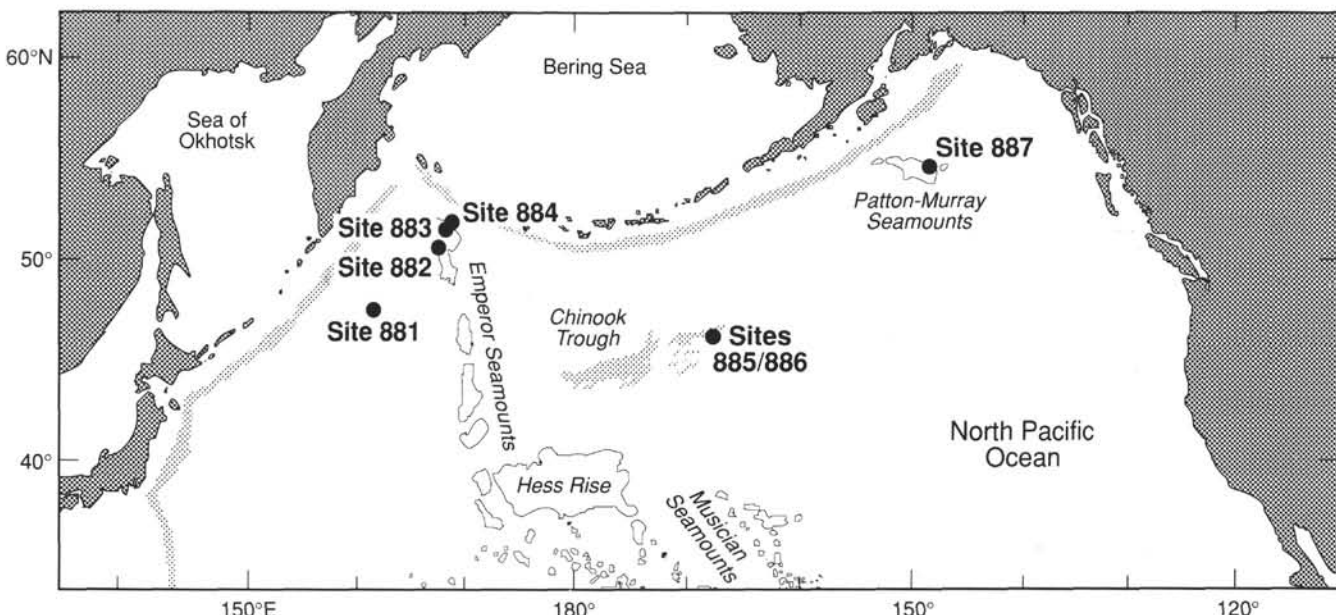


Figure 1. Index map of North Pacific showing locations of Leg 145 drill sites.

Maruyama (1992), and Akiba et al. (1993) and is summarized in the Appendix. The reader should also consult Gladenkov and Barron (this volume) for taxonomic citations and illustrations of the Oligocene through early middle Miocene taxa discussed.

Because we were not certain how to separate selected taxa of *Crucidenticula* and *Denticulopsis* that have been proposed by Yanagisawa and Akiba (1990), we have made the following groupings:

*Crucidenticula nicobarica* = *C. paranicobarica* and *C. nicobarica*;  
*Denticulopsis hustedtii* = *D. hustedtii*, *D. simonsenii*, *D. vulgaris*, and *D. praekatayamae*;  
*D. hyalina* = *D. hyalina* and *D. miocenica*;  
*D. lauta* = *D. lauta*, *D. ichikawai*, *D. okunoi*, *D. tanimurae*, and *D. praehyalina*.

### Time Scale

Absolute ages throughout the paper are updated according to the geomagnetic polarity time scale of Cande and Kent (1992). Correlation of the geologic epochs and periods used follows that of Berggren et al. (1985a, 1985b), with the exception of the Miocene/Pliocene boundary, in which the calibration of Zijderveld et al. (1986) is used.

### Zonation

The diatom zonation used for the middle Miocene through Quaternary (Fig. 2) closely follows the zonation of Akiba (1986) with two changes: (1) the last occurrence (LO) of *Neodenticula koizumii* is used to define the base of the *Actinocyclus oculus* Zone, as suggested by Koizumi (1992); and (2) the *Neodenticula kamtschatica* Zone is used in its traditional sense, that is, as the interval from the first occurrence (FO) of *N. kamtschatica* s. str. to the FO of *N. koizumii*. The *N. kamtschatica* Zone is divided into Subzones a, b, and c by the FO of *Thalassiosira oestrupii* and the LO of *T. insigna* after Barron (1980a).

Below the early middle Miocene *Denticulopsis praelauta* Zone of Akiba (1986), a series of partial-range zones are proposed for the Oligocene and early Miocene by Gladenkov and Barron (this volume) based on the successive (downhole) FO of *Crucidenticula kanayaee*, *C. sawamuriae*, *Thalassiosira fraga*, *T. praefraga*, *Rocella gelida*, *Cavatitus rectus*, and *R. vigilans*.

## RESULTS

The diatom biostratigraphy of the Leg 145 sites is discussed in order of decreasing temporal length of the available paleomagnetic stratigraphic record. Consequently, Site 887 is discussed first, followed in turn by Sites 884, 882, 883, and 881.

### Site 887

Four holes were drilled at Site 887 (54°21.9'N, 148°26.8'W; water depth, 3645 m) on the Patton-Murray Seamount in the northeast Pacific (Shipboard Scientific Party, 1993e). Diatoms generally are common to abundant, with preservation ranging from good to poor in the lower Miocene to Pleistocene section cored above about 280 mbsf at the site (Fig. 3; Core 145-887D-3R).

Paleomagnetic stratigraphy at the site extended without interruption back to magnetic polarity Subchron C5En (Shipboard Scientific Party, 1993e). Except for parts of the early Miocene and early middle Miocene, all of the diatom assemblages are readily zonable by the Leg 145 North Pacific diatom zonation (Fig. 3), and standard North Pacific diatom datum levels are recognizable from the late early Miocene *Crucidenticula sawamuriae* Zone through the late Pleistocene *Neodenticula seminaiae* Zone (Table 1).

The estimated ages of early Miocene to late Pliocene diatom datum levels at Site 887 are based on the magnetostratigraphy and are shown in parentheses in Table 1. Other age estimates are from the literature. A correlation of gamma-ray attenuation porosity evaluator (GRAPE) events between Holes 887A and 887C (see note to Table 1) was used to reconcile the stratigraphic differences between the two holes. These ages will be discussed in detail later in the paper, where they will be compared with those derived from the magnetostratigraphy at other Leg 145 sites.

In contrast to the sites from the northwest Pacific (Sites 881 to 884), Pleistocene assemblages (Cores 145-887A-1H through -8H, 145-887B-1H through -5H; and 145-887C-1H through -9H) typically are very well preserved and easily zonable. Reworking seems to be minimal with the exception of Sample 145-887B-4H-CC, where common *Actinocyclus oculus*, which is typical of the early part of the Pleistocene, is reworked into the upper Pleistocene *Simonsenella curvirostris* Zone. Reworking is likely, because older Sample 145-

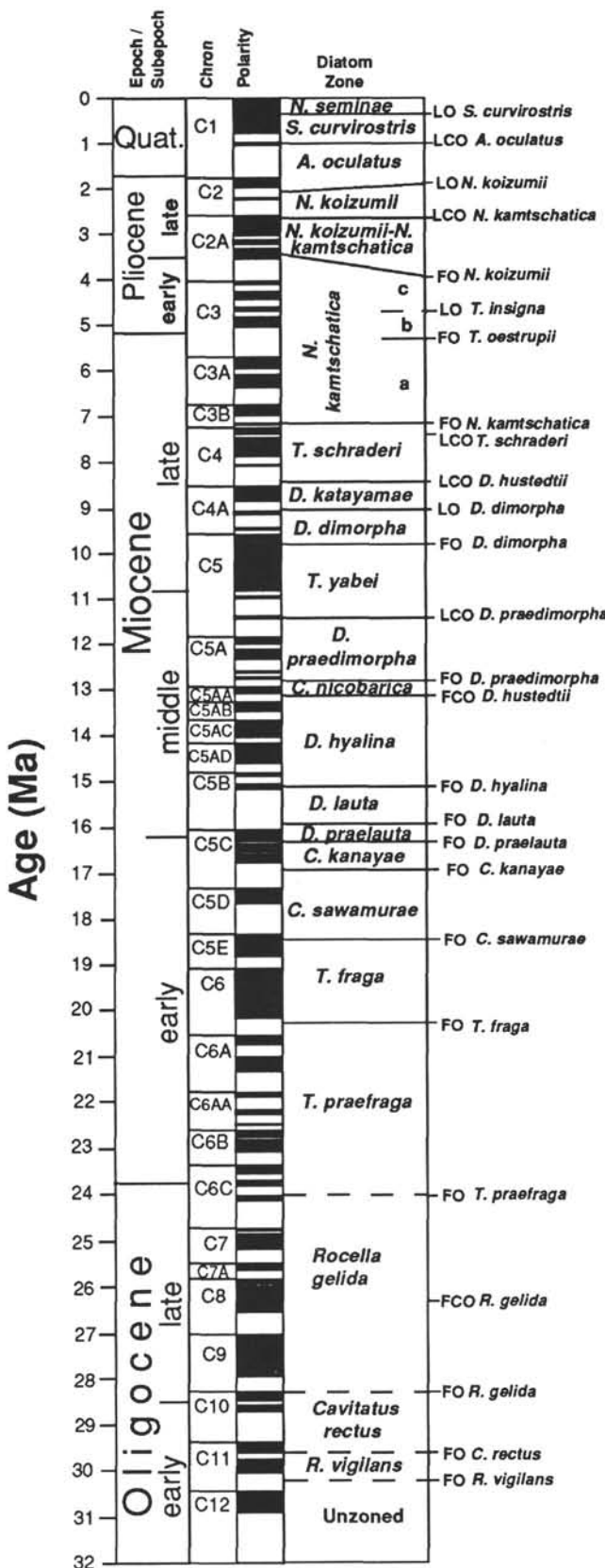


Figure 2. The Oligocene to Quaternary diatom zonation used for Leg 145 (modified from Akiba [1986] and Koizumi [1992] and proposed by Gladenkov and Barron [this volume]), correlated to the geomagnetic polarity time scale of Cande and Kent (1992). LO = last occurrence, LCO = last common occurrence, FO = first occurrence, and FCO = first common occurrence.

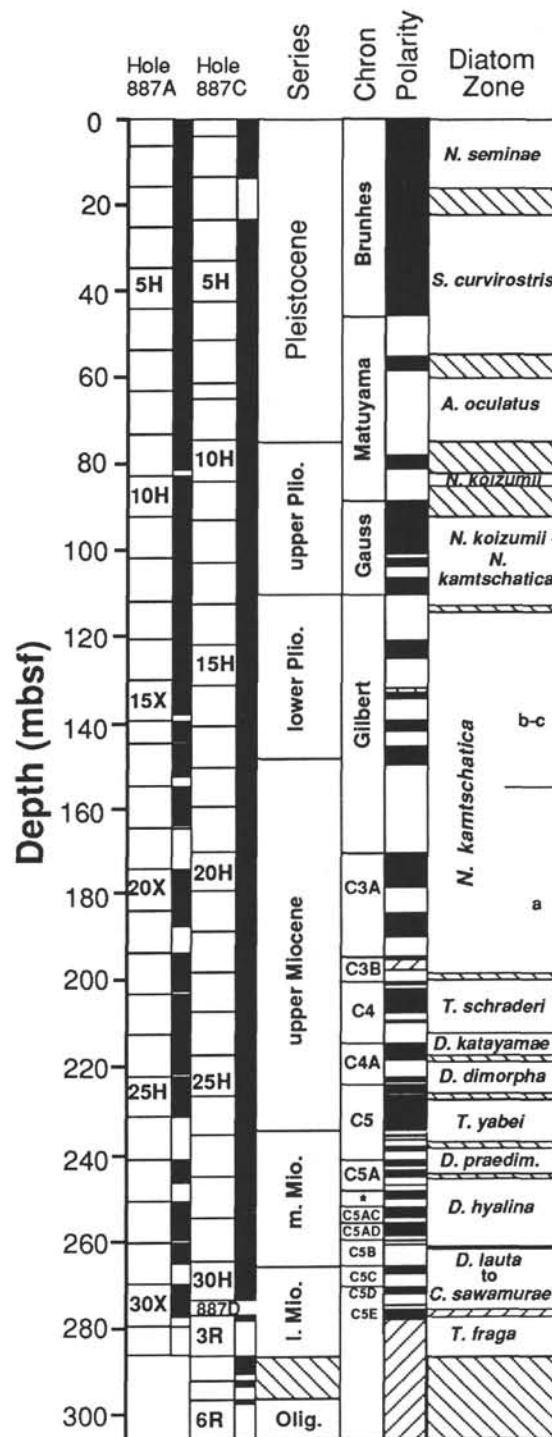


Figure 3. Stratigraphic position of cores, recovery (black), ages, placement of magnetostratigraphic chronos and subchrons, polarity log, and placement of diatom zones in Holes 887A, 887C and 887D. Intervals filled by slanted lines indicate uncertainty in the placement of biostratigraphic boundaries and/or absence of paleomagnetic stratigraphy. The magnetostratigraphy shown (Shipboard Scientific Party, 1993e) is that of Hole 887A for the interval 5–0 Ma and that of Hole 887C for older intervals. The plotted depths of magnetostratigraphic events are adjusted to conform to Hole 887A using the following correlation: GRAPE events in Hole 887A at 161.3, 201.2, 214.2, 230.6, and 256.9 mbsf correspond respectively to events at 160.0, 199.5, 211.8, 227.6, and 253.2 mbsf in Hole 887C. H = hydraulic piston core, X = extended core barrel, and R = rotary core barrel.

**Table 1.** Age and stratigraphic position of late early Miocene through Quaternary diatom datum levels and magnetic polarity events in Holes 887A and 887C.

Datum	Age (Ma)	Source	Hole 887A		Hole 887C	
			Interval	Depth (mbsf)	Interval	Depth (mbsf)
LO <i>Simonsenella curvirostris</i>	0.3	2	2H-CC/3H-CC	16.2/25.7 45.55 55.6	2H-CC/3H-CC	13.8/23.3 42.7 52.6
B C1n.1n	0.78					
T C1r.1n	0.984					
LCO <i>Actinocyclus oculus</i>	1.0	1	6H-CC/7H-CC	54.2/63.7 58.95	6H-CC/7H-CC	51.8/61.3 56.25
B C1r.1n	1.049					
FO <i>Simonsenella curvirostris</i>	1.58	1	7H-CC/8H-CC	63.7/73.2	9H-CC/10H-CC	74.3/83.8 75.35
T C2n.1n	1.757					
B C2n.1n	1.983					
LO <i>Neodenticula koizumii</i>	2.0	2	8H-CC/9H-CC	73.2/82.7 88.9	9H-CC/10H-CC	74.3/83.8 87.3
T C2An.1n	2.6					
LCO <i>Neodenticula kamtschatica</i>	2.63–2.7	1	9H-CC/10H-CC	82.7/92.2 101.1	10H-CC/11H-CC	83.8/93.3 98.3
FO <i>Neodenticula seminae</i>	2.7	1	9H-CC/10H-CC	82.7/92.2 101.85	10H-CC/11H-CC	83.8/93.3 100.55
B C2An.1n	3.054					
T C2An.2n	3.127					
B C2An.2n	3.221					
LO <i>Thalassiosira marujamica</i>	(3.25)		12H-2, 135 cm/12H-3, 5 cm	104.55/104.75	11H-CC/12H-CC	93.3/103.8
T C2An.3n	3.325					
B C2An.3n	3.553					
FO <i>Actinocyclus oculus</i>	(3.65)		13H-1, 21 cm/13H-2, 21 cm	111.4/112.9		
FO <i>Neodenticula koizumii</i>	(3.70)		13H-2, 21 cm/13H-3, 21 cm	112.9/114.4	13H-CC/14H-CC	112.3/121.8
T C3n.1n	4.033					
B C3n.1n	4.134					
B C3n.2n	4.432					
T C3n.3n	4.611					
B C3n.3n	4.694			134.7 142.2		134.8 139.65
LO <i>Thalassiosira jacksonii</i> (plicate)	(4.8)		16X-CC/17X-1, 21 cm	144.37/145.3		
T C3n.4n	4.812					
B C3n.4n	5.046					
FO <i>Thalassiosira latimarginata</i>	(5.0)		17X-3, 21 cm/17X-4, 21 cm	148.3/149.8	17H-CC/18H-CC	150.3/159.8
FO <i>Thalassiosira jacksonii</i> (plicate)	(5.0)		17X-3, 21 cm/17X-4, 21 cm	148.3/149.8	17H-CC/18H-CC	150.3/159.8
FO <i>Thalassiosira oestrupii</i>	(5.3*)		17X-CC/18X-1, 21 cm	154.8/155.0	17H-CC/18H-CC	150.3/159.8
T C3An.1n	5.705					
LO <i>Thalassiosira miocenica</i>	(5.9*)		20X-2, 21 cm/20-3, 21 cm	175.8/177.3	19H-CC/20H-CC	169.3/178.8
B C3An.1n	5.946					
T C3An.2n	6.078					
FO <i>Thalassiosira miocenica</i>	(6.2*)		21X-1, 22 cm/21X-2, 22 cm	183.9/185.4	20H-CC/21H-CC	178.8/188.3
LO <i>Cavitatus jouseana</i>	(6.6*)		21X-CC/22H-1, 25 cm	193.4/193.6		
B C4n.1n	7.376					
FO <i>Neodenticula kamtschatica</i>	(7.1–7.2*)		22H-4, 21 cm/22H-5, 21 cm	198.1/199.6	22H-CC/23H-CC	197.8/207.3
FO <i>Nitzschia reinholdii</i>	(7.2–7.3*)		22H-5, 21 cm/22H-6, 21 cm	199.6/201.1		
LCO <i>Thalassionema schraderi</i>	(7.4–7.5*)		22H-6, 21 cm/22H-CC	201.1/202.9	22H-CC/23H-CC	197.8/207.3
T C4n.2n	7.464					
B C4n.2n	7.892					
T C4r.1n	8.047					
LO <i>Denticulopsis katayamae</i>	(8.1–8.2*)		23H-5, 21 cm/23H-6, 21 cm	209.1/210.6		
LO <i>Thalassiosira minutissima</i>	(8.2–8.3*)		23H-6, 21 cm/23H-7, 21 cm	210.6/212.1		
LCO <i>Denticulopsis hustedtii</i>	(8.4*)		23H-7, 21 cm/23H-CC	212.1/212.4	23H-CC/24H-CC	207.3/216.8
T C4An.1n	8.529					
B C4An.1n	8.861					
LO <i>Denticulopsis dimorpha</i>	(8.8–8.9*)		24H-4, 21 cm/24H-5, 21 cm	217.1/218.6	23H-CC/24H-CC	207.3/216.8
FO <i>Denticulopsis katayamae</i>	(9.4*)		24H-CC/25H-1, 21 cm	221.9/222.1		
FO <i>Thalassinema schraderi</i>	(9.4*)		24H-CC/25H-1, 21 cm	221.9/222.1		
FO <i>Thalassiosira minutissima</i>	(9.4*)		24H-CC/25H-1, 21 cm	221.9/222.1		
T C4r.2n	9.428					
B C4Ar.2n	9.491					
FO <i>Thalassionema robusta</i>	(9.5*)		25H-1, 21 cm/25H-2, 24 cm	222.1/223.6	24H-CC/25H-CC	216.8/223.3
LO <i>Simonsenella praebarboi</i>	(9.5*)		25H-1, 21 cm/25H-2, 24 cm	222.1/223.6		
T C5n.1n	9.592					
B C5n.1n	9.735					
T C5n.2n	9.777					
FO <i>Denticulopsis dimorpha</i>	(9.8–9.9*)		25H-3, 133 cm/25H-4, 133 cm	226.23/227.73	24H-CC/25H-CC	216.8/223.3
FO <i>Hemidiscus cuneiformis</i>	(10.4–10.6)		26H-2, 21 cm/26H-2, 21 cm	228.0/229.5		
LO <i>Nitzschia heteropolica</i>	(10.6–10.8)		26H-3, 21 cm/26H-4, 21 cm	229.5/231.0		
B C5n.2n	10.834					
T C5r.2n	11.378					
LCO <i>Denticulopsis praedimorpha</i>	(11.2–11.4)		25H-CC/27H-1, 60 cm	231.4/241.8	26H-6, 21 cm/26H-7, 21 cm	234.0/235.5
LO <i>Mediaria splendida</i>	(11.4–11.5)		25H-CC/27H-1, 60 cm	231.4/241.8	26H-7, 21 cm/26H-CC	235.5/235.8
T C5An.1n	11.852					
B C5An.1n	12.00					
T C5An.2n	12.108					
B C5An.2n	12.333					
FO <i>Simonsenella barboi</i>	(12.0–12.4*)		25H-CC/27H-1, 60 cm	231.4/241.8	27H-3, 21 cm/27H-6, 21 cm	239.0/243.5
FO <i>Nitzschia heteropolica</i>	(12.4–12.6*)		27H-1, 60 cm/27H-2, 20 cm	241.8/242.9		
LO <i>Crucidenticula nicobarica</i>	(12.4–12.6*)		27H-1, 60 cm/27H-2, 20 cm	241.8/242.9		
FO <i>Denticulopsis praedimorpha</i>	(12.7–13.1)		27H-3, 20 cm/27H-3, 124 cm	244.4/245.44	27H-6, 21 cm/27H-CC	243.5/245.3
FCO <i>Denticulopsis hustedtii</i>	(12.7–13.1)		27H-3, 20 cm/27H-3, 124 cm	244.4/245.44	27H-6, 21 cm/27H-CC	243.5/245.3
T C5ACn.1n	13.674					
B C5ACn.1n	14.059					
T C5ADn.1n	14.164					
FO <i>Denticulopsis hustedtii</i>	(13.6–14.6*)		27H-CC/28H-CC	250.7/260.2	27H-CC/28H-CC	245.3/254.8
T C5Bn.1n	14.8					
B C5Bn.1n	14.89					
FO <i>Denticulopsis hyalina</i>	(14.9–15.1*)		29H-1, 51 cm/29H-2, 21 cm	260.7/261.9	?27H-CC/28H-CC	245.3/254.8
T C5Bn.2n	15.038					
B C5Bn.2n	15.162					
FO <i>Actinocyclus ingens nodus</i>	(15.5–16.7*)		29H-4, 21 cm/29H-CC	264.1/269.7	28H-CC/29H-CC	254.8/264.3
T C5Cn.1n	16.035					262.1

Table 1 (continued).

Datum	Age (Ma)	Source	Hole 887A		Hole 887C	
			Interval	Depth (mbsf)	Interval	Depth (mbsf)
FO	<i>Denticulopsis lauta</i>	15.9	3	30X-5, 90 cm/30X-CC	276.6/279.4	
FO	<i>Denticulopsis praelauta</i>	16.2	3	Not seen	Not seen	
FO	<i>Crucidenticula kanayae</i>	(16.7–17.1)			30H-1, 21 cm/30H-2, 21 cm	264.51/266.01
T	C5Dn.1n	17.31				266.75
B	C5Dn.1n	17.65				268.4
T	C5En.1n	18.317				271.95
FO	<i>Crucidenticula sawamurae</i>	(18.3–18.5)		>30X-CC	30H-6, 21 cm/30H-7, 21 cm	272.0/273.7
FO	<i>Thalassiosira fraga</i>	20.1	4		<30H-CC	<273.8

Notes: Magnetostratigraphy is after Shipboard Scientific Party (1993e). Ages and polarity subchron terminology are according to the Cande and Kent (1992) geomagnetic polarity time scale. Interpolated ages of diatom datum based on Site 887 magnetostratigraphy are shown in parentheses; other datum level ages are from the following sources: 1 = Koizumi and Tanimura (1985); 2 = Koizumi (1992); 3 = Barron (1992); and 4 = Baldauf and Barron (1991). Samples constraining each datum level are separated by a (/) as are the meters below seafloor (mbsf) of these samples. LO = last occurrence; LCO = last common occurrence; FO = first occurrence; FCO = first common occurrence; B = base; and T = top. The plotted depths of magnetostratigraphic events are adjusted to conform to Hole 887A using the following correlations: GRAPE events in Hole 887A at 161.3, 201.2, 214.2, 230.6, and 256.9 mbsf correspond respectively to events at 160.0, 199.5, 211.8, 227.6, and 253.2 mbsf in Hole 887C.

887B-5H-CC contains an assemblage lacking *A. oculus* and assignable to the *S. curvirostris* Zone and because diatom biostratigraphy at equivalent depths in Hole 887A is supportive of such a zonal assignment (Table 1). Diatom datum levels from Hole 887B, which recovered only five cores, are not reported here (see Shipboard Scientific Party, 1993e).

Persistent reworking of middle Miocene forms of *Actinocyclus ingens* and *A. ingens* var. *nodus* was documented in the upper Miocene and Pliocene sediments of Hole 887C (Cores 145-887C-11H through -23H; 84–207 mbsf). Hole 887A also contains reworked middle Miocene taxa in the upper Miocene and Pliocene section, but they were not documented as thoroughly as those of Hole 887C. Reworked specimens typically are rare (<2% of the assemblage), but in Sample 145-887C-23H-CC, they are relatively common (perhaps 5% to 10% of the assemblage).

The middle Miocene *Crucidenticula nicobarica* Zone may be missing at an unconformity near 245 mbsf in Hole 887A. Sample 145-887A-27H-3, 20 cm (244.4 mbsf), contains *Denticulopsis praedimorpha* and common *D. hustedtii* and is assignable to the *D. praedimorpha* Zone (11.4–12.8 Ma), whereas the dominance of *D. hyalina* over *D. hustedtii* without *D. praedimorpha* in Sample 145-887A-27H-3, 124 cm (245.44 mbsf), argues for correlation of that sample with the *Denticulopsis hyalina* Zone (13.1–15.1 Ma).

Although *Denticulopsis lauta* was not recorded in Sample 145-887C-28H-CC (254.8 mbsf), the presence of *Actinocyclus ingens* var. *nodus* in that sample indicates an age no older than the *D. lauta* Zone. Although poorly preserved Sample 145-887A-29H-CC (264.3 mbsf) also lacks *Denticulopsis lauta*, this taxon does occur in Sample 145-887A-29H-CC (269.7 mbsf), suggesting the possibility that *D. lauta* has been selectively removed from the former sample.

The FO of *Crucidenticula sawamurae* in Sample 145-887C-30H-6, 21 cm (272.0 mbsf), is correlative with the uppermost part of a normal polarity event that appears to be Chron C5En (Shipboard Scientific Party, 1993e). Thus the FO of *C. sawamurae* at Site 887 is slightly older than the Chron C5Dn correlation reported by Barron (1985a) (as *C. nicobarica*) at equatorial Pacific DSDP Site 575; however, it is in accord with the correlations of Baldauf et al. (1987) at DSDP Site 610 in the North Atlantic.

Samples 145-887C-30H-CC (273.8 mbsf) and 145-887D-3R-CC (286.7 mbsf) contain a low-diversity early Miocene assemblage of *Stellarima* spp., *Cavatatus jouseanus*, and *Coscinodiscus marginatus* and are not readily zonable. The presence of the silicoflagellate *Naviculopsis lata obliqua* in these samples, however, indicates that they are likely to be equivalent to the *Thalassiosira fraga* Zone, as that silicoflagellate was found to be restricted to the *T. fraga* Zone at Sites 883 and 884 (Bukry, this volume; A. Gladenkov, unpubl. data). The absence of *Thalassiosira fraga* in these samples is assumed to be caused by ecological exclusion.

## Site 884

Drilling at Site 884 on the east flank of Detroit Seamount in the northwest Pacific (51°27'N, 168°20.2'E; water depth, 3836 m) recovered an 850-m sequence of upper Paleocene(?) through Pleistocene sediments in five holes (Shipboard Scientific Party, 1993d). In general, diatoms are abundant to common and well preserved to moderately well preserved throughout the upper Oligocene through Quaternary section cored above 658 mbsf at Site 884 (see also Gladenkov and Barron, this volume).

A complete sequence of all of the Neogene North Pacific diatom zones from the early Oligocene *Roccella vigilans* Zone through the late Quaternary *Neodenticula seminae* Zone was cored at Site 884 (Fig. 4). The reader is referred to Gladenkov and Barron (this volume) for detailed documentation of diatom occurrences in the older part of Hole 884B. Standard diatom datum levels are used to recognize these zones (Table 2) and little or no displacement of diatom biostratigraphic levels is apparent between Holes 884B and 884C.

At Site 884, sediments correlative to the upper middle Miocene *Thalassiosira yabei* Zone and lowermost Miocene *Thalassiosira praefraga* and uppermost Oligocene *Roccella gelida* Zones were recovered; these same intervals, however, are either missing or greatly compressed at Site 883. An added bonus of drilling at Site 884 was the recording of an excellent paleomagnetic stratigraphy in the upper 560 m of Hole 884B, which extends from the Pleistocene back to at least the early middle Miocene or more (Fig. 4).

The magnetostratigraphy of the middle Miocene through Quaternary sequence in Hole 884B follows "Interpretation 2" of the Shipboard Scientific Party (1993d), with the following modification: the normal polarity interval recognized between 535.0 and 542.3 mbsf is assigned to combined Subchrons C5AA and C5AB, whereas the normal interval recognized between 550 and 559 mbsf is assigned to Subchron C5AC. These modifications are based on diatom-magnetostratigraphic correlations at Site 887 (Fig. 3), where the magnetostratigraphic record is easier to interpret. In addition, shipboard measurement of inclination from the pass-through cryogenic magnetometer (after 15 mT demagnetization) identified normal polarity intervals beginning at 580.0, 594.2, and 602.8 mbsf that are tentatively correlated with the tops of Chrons C5C, C5D, and C5E, respectively (Table 2; Fig. 4).

The absolute ages of early Miocene to Pleistocene diatom datum levels that are estimated at Site 884 based on the magnetostratigraphy are shown in parentheses in Table 2. These ages will be discussed later in the paper.

In contrast to the overwhelmingly holoplanktonic character of the diatom assemblages observed in uppermost Miocene through Quaternary section of Sites 882 and 883 on the top of Detroit Seamount, diatom assemblages in correlative sediments at Site 884 contain con-

Table 2. Age and stratigraphic position of late early Miocene through Quaternary diatom datum levels and magnetic polarity events in Holes 884B and 884C.

Datum	Age (Ma)	Source	Hole 884B		Hole 884C	
			Interval	Depth (mbsf)	Interval	Depth (mbsf)
LO <i>Simonsenella curvirostris</i>	0.3	2	1H-CC/2H-CC	6.5/16.0	2H-CC/3H-CC	11.9/21.4
LO <i>Thalassiosira jouseae</i>	0.3–0.41		1H-CC/2H-CC	6.5/16.0		
B C1n.1n	0.78			42.5		41.1
T C1r.1n	0.984					55
LCO <i>Actinocyclus oculatus</i>	(0.9–1.0)		5H-CC/6H-CC	44.5/54.0	6H-CC/7H-CC	49.9/59.4
B C1r.1n	1.0			59.4		59.7
FO <i>Simonsenella curvirostris</i>	1.58	1	11H-CC/12X-CC	87.3/93.3	10X-CC/11X-CC	88.2/97.8
B C2n.1n	1.983			96.9		101.9
LO <i>Pyxidicula horridus</i>	(1.8–2.0)		12X-CC/13X-4, 54 cm	93.3/98.34	12X-CC/13X-CC	107.4/117.0
LO <i>Pyxidicula pustulata</i>	(2.0–2.2)		13X-4, 54 cm/14X-4, 47 cm	98.34/108.97		
LO <i>Neodenticula koizumii</i>	(2.0–2.2)		13X-4, 54 cm/14X-4, 47 cm	98.34/108.97	11X-CC/12X-CC	97.8/107.4
LO <i>Pyxidicula zabelinae</i>	(2.0–2.2)		13X-CC/14X-4, 47 cm	98.5/108.97		
T C2An.1n	2.6			121.30–122.50		
LCO <i>Neodenticula kamtschatica</i>	2.63–2.7	1	15X-CC/16X-CC	122.2/131.8	15X-CC/16X-CC	136.3/146.0
FO <i>Neodenticula seminae</i>	2.7	1	15X-CC/16X-CC	122.2/131.8	15X-CC/16X-CC	136.3/146.0
B C2An.1n	3.054			148.1		147.00–147.80
T C2An.2n	3.127			152.35		154.50–156.00
LO <i>Thalassiosira marujamica</i>	(3.1–3.2)		18X-CC/19X-CC	151.0/160.8	17X-CC/18X-CC	155.7/165.3
B C2An.2n	3.221			159.5–159.7		158.5–159.5
T C2An.3n	3.325					164.4
B C2An.3n	3.553			179.2		178
LO <i>Thalassiosira jacksonii</i>	(3.7–3.8)		23X-5, 25 cm/23X-CC	196.05/199.4	21X-CC/22X-CC	194.3/204.0
FO <i>Neodenticula koizumii</i>	(3.7–3.8)		23X-5, 25 cm/23X-CC	196.05/199.4	21X-CC/22X-CC	194.3/204.0
FO <i>Actinocyclus oculatus</i>	(3.9)		24X-5, 25 cm/24X-CC	205.65/209.1	22X-CC/23X-CC	204.0/213.7
T C3n.1n	4.033			219.65		218.45
B C3n.1n	4.134			224.2		224.5
T C3n.2n	4.265					235.9
B C3n.2n	4.432					244.25
T C3n.3n	4.611			252.1?		251.5–252.4
B C3n.3n	4.694			258.4?		256.9
LO <i>Thalassiosira jacksonii</i> (plicate)	(4.6)		29X-CC/30X-2, 25 cm	252.4/259.05	28X-CC/29X-CC	261.8/271.4
LO <i>Thalassiosira insignia</i>	(4.7–4.8)		30X-5, 25 cm/30X-CC	263.55/267.0		
T C3n.4n	4.812			266.3–267.9		261.8–261.9
FO <i>Thalassiosira tertaria</i>	(4.85)		30X-CC/31X-2, 25 cm	267.0/268.75		
FO <i>Thalassiosira latimarginata</i> s.str.	(4.9)		31X-2, 25 cm/31X-5, 25 cm	268.75/273.25	29X-CC/30X-CC	271.4/281.1
B C3n.4n	5.046			276.5–276.9		
FO <i>Thalassiosira jacksonii</i> (plicate)	(5.0)		31X-CC/32X-2, 25 cm	276.7/278.45		
FO <i>Thalassiosira latimarginata</i> s.ampl.	(5.3)		33X-2, 25 cm/33X-5, 25 cm	288.05/292.55		
FO <i>Thalassiosira oestrupii</i>	(5.3)		33X-2, 25 cm/33X-5, 25 cm	288.05/292.55	30X-CC/31X-CC	281.1/290.7
LO <i>Ikebea tenuie</i>	(5.4–5.5)		34X-2, 25 cm/34X-CC	297.75/304.7		
T C3An.1n	5.705			311.55		
LO <i>Nitzschia suikoensis</i>	(5.7–5.75)		35X-5, 25 cm/35X-CC	311.95/315.3		
LO <i>Rouxia californica</i>	(5.7–5.75)		35X-5, 25 cm/35X-CC	311.95/315.3		
LO <i>Thalassiosira miocenica</i>	(5.8)		35X-CC/36X-2, 25 cm	315.3/317.05	34X-CC/35X-CC	319.7/329.2
LO <i>Thalassiosira singularis</i>	(5.8)		35X-CC/36X-2, 25 cm	315.3/317.05		
FO <i>Thalassiosira praeoestrupii</i>	(5.95)		36X-5, 25 cm/36X-CC	321.55/325.0	34X-CC/35X-CC	319.7/329.2
B C3An.1n	5.946			324.8–325.2		325.7
FO <i>Thalassiosira convexa aspinosa</i>	(6.1)		37X-5, 25 cm/37X-CC	331.25/334.3		
T C3An.2n	6.078			334.5		332.4
FO <i>Thalassiosira manifesta</i>	(6.2)		38X-2, 25 cm/38X-5, 25 cm	336.05/340.55		
FO <i>Thalassiosira miocenica</i>	(6.2)		38X-2, 25 cm/38X-5, 25 cm	336.05/340.55	36X-CC/37X-CC	338.7/348.2
B C3An.2n	6.376			348		348.2
FO <i>Thalassiosira jacksonii</i>	(6.5–6.6)		40X-2, 24 cm/40X-5, 24 cm	355.34/359.84		
LO <i>Cavitatus jouseanus</i>	(6.5–6.6)		40X-2, 24 cm/40X-5, 24 cm	355.34/359.84		
T C3Bn.1n	6.744			364.0–364.6		
B C3Bn.1n	6.901			367.6		
FO <i>Thalassiosira marujamica</i>	(6.8–6.9)		41X-2, 25 cm/41X-5, 25 cm	364.85/369.36		
T C3Br.1n	6.946			369.1		
B C3Br.1n	6.981			370.25		
FO <i>Neodenticula kamtschatica</i>	(7.1–7.2)		41X-CC/42X-2, 26 cm	372.7/374.46		
T C4n.1n	7.245			374.2		
B C4n.1n	7.376			379.65		
LCO <i>Thalassionema schraderi</i>	(7.35–7.45)		42X-5, 25 cm/42X-CC	378.95/382.4		
T C4n.2n	7.464			381.5		
FO# <i>Actinocyclus curvatulus</i>	(7.5–7.6)		43X-2, 25 cm/43X-5, 25 cm	384.15/388.65		
FO <i>Nitzschia pliocena</i>	(7.6–7.7)		43X-5, 25 cm/44X-2, 25 cm	388.65/393.75		
FO <i>Nitzschia fossilis</i>	(7.6–7.7)		43X-5, 25 cm/44X-2, 25 cm	388.65/393.75		
FO <i>Nitzschia rolandii</i>	(7.8–7.9)		44X-2, 25 cm/44X-5, 25 cm	393.75/398.25		
FO# <i>Thalassiosira gravida</i>	(7.9–8.0)		44X-5, 25 cm/44X-2, 25 cm	398.25/403.45		
FO <i>Thalassiosira singularis</i>	(7.9–8.0)		44X-5, 25 cm/44X-2, 25 cm	398.25/403.45		
B C4n.2n	7.892			400.2		
FO <i>Nitzschia praereinholdii</i>	(8.3)		46X-2, 25 cm/46X-3, 25 cm	413.05/414.55		
LCO <i>Denticulopsis katayamae</i>	(8.4)		46X-3, 25 cm/46X-4, 25 cm	414.45/416.05		
FO <i>Nitzschia suikoensis</i>	(8.4)		46X-3, 25 cm/46X-4, 25 cm	414.45/416.05		
T C4An.1n	8.529			418.45		
B C4An.1n	8.861			436.15		
LO <i>Denticulopsis dimorpha</i>	(9.0)		48X-6, 25 cm/48X-CC	438.35/440.2		
T C4Ar.1n	9.069			440.65		
FO <i>Thalassiosira minutissima</i>	(9.1)		49X-2, 25 cm/49X-3, 25 cm	441.95/443.45		
FO <i>Denticulopsis katayamae</i>	(9.1)		49X-3, 25 cm/49X-4, 25 cm	443.45/444.95		
T C4Ar.1n	9.149			445.2		
LO <i>Denticulopsis crassa</i>	(9.3)		49X-6, 25 cm/49X-7, 25 cm	447.95/449.45		
FO <i>Thalassionema schraderi</i>	(9.3)		49X-6, 25 cm/49X-7, 25 cm	447.95/449.45		
T C4r.2n	9.428			451.1?		
B C4r.2n	9.491			453.1?		
T C5n.1n	9.592			453.9?		
B C5n.1n	9.735			457.3?		

Table 2 (continued).

Datum	Age (Ma)	Source	Hole 884B		Hole 884C	
			Interval	Depth (mbsf)	Interval	Depth (mbsf)
T C5n.2n	9.777			458.0–459.5?		458.0
FO <i>Denticulopsis dimorpha</i>	(9.8)		50X-CC/51X-2, 27 cm	459.3/461.07		
FO <i>Hemidiscus cuneiformis</i>	(10.7–10.9)		54X-CC/55X-CC	497.8/507.4		
LO <i>Nitzschia heteropolica</i>	(10.7–10.9)		54X-CC/55X-CC	497.8/507.4		
LO <i>Mediaria splendida</i>	(10.7–10.9)		54X-CC/55X-CC	497.8/507.4		
B C5n.2n	10.834			498.0–507.0		
LCO <i>Denticulopsis praedimorpha</i>	(11.4)		56X-2, 25 cm/56X-4, 25 cm	509.15/512.15		
T C5An.1n	11.852			520.7		
B C5An.1n	12.000			522.1		
T C5An.2n	12.108			523.0		
B C5An.2n	12.333			525.5		
FO <i>Simonsenella barboi</i>	(12.4)		57X-CC/58X-2, 25 cm	526.7/528.45		
T C5Ar.1n	12.618			528.5		
B C5Ar.1n	12.649			530.00		
T C5Ar.2n	12.718			531.00		
B C5Ar.2n	12.764			532.50		
LO <i>Crucidenticula nicobarica</i>	(12.8)		58X-5, 25 cm/58X-6, 25 cm	532.75/534.25		
FO <i>Denticulopsis praedimorpha</i>	(12.8)		58X-5, 25 cm/58X-6, 25 cm	532.75/534.25		
FCO <i>Denticulopsis hustedtii</i>	(13.1)		58X-7, 25 cm/58X-CC	535.75/536.4		
T C5AAn.1n	12.941			535.00		
FO <i>Nitzschia heteropolica</i>	(13.1–13.2)		58X-CC/59X-2, 25 cm	536.4/538.15		
B C5ABn.1n*	13.476			542.3		
T C5Cn.1n*	13.674			550		
T C5Cn.1n*	14.059			559		
FO <i>Denticulopsis hustedtii</i>	14.2	4	60X-CC/61X-CC	555.6/565.3		
FO <i>Denticulopsis hyalina</i>	(15.1)		62X-4, 25 cm/62X-6, 25 cm	567.05/570.05		
FO <i>Cavatina lanceolatus</i>	(15.6)		62X-CC/63X-2, 25 cm	574.8/576.55		
FO <i>Actinocyclus ingens nodus</i>	(15.8)		63X-2, 25 cm/63X-4, 25 cm	576.55/579.55		
T C5Cn.1n?	16.035			580.0		
FO <i>Denticulopsis lauta</i>	(15.9)	3	63X-3, 25 cm/63X-4, 25 cm	578.05/579.55		
LO <i>Crucidenticula kanayae</i>	(16.2)		63X-6, 25 cm/63X-CC	582.55/583.83		
FO <i>Denticulopsis praelauta</i>	(16.3)		63X-CC/64X-1, 25 cm	583.83/584.65		
FO <i>Nitzschia challengerii</i>	(16.3)		63X-CC/64X-1, 25 cm	583.83/584.65		
LO <i>Crucidenticula sawamuriae</i>	(16.6)		64X-2, 25 cm/64X-3, 25 cm	586.15/587.65		
FO <i>Crucidenticula kanayae</i>	(16.9)		64X-4, 28 cm/64X-5, 25 cm	589.15/590.65		
T C5Dn.1n?	17.31			594.2		
B C5Dn.1n?	17.65			599.0		
FO <i>Mediaria splendida</i>	(17.8)		65X-4, 25 cm/65X-6, 25 cm	598.85/601.85		
T C5En.1n	18.317			602.8		
FO <i>Crucidenticula sawamuriae</i>	(18.4)		65X-CC/66X-1, 25 cm	603.8/604.05		
LO <i>Thalassiosira praefraga</i>	(18.4)		65X-CC/66X-1, 25 cm	603.8/604.05		
O <i>Nitzschia maleinterpretaria</i>	(18.5–18.6)		66X-2, 25 cm	605.55		
B C6n.1n?	20.162			610.0		
FO <i>Thalassiosira fraga</i>	20.1 (20.3)	3	66X-5, 25 cm/66X-6, 25 cm	610.05/611.55		

Notes: See Gladenkov and Barron (this volume) for older datum levels. Magnetostratigraphy is after Shipboard Scientific Party (1993d) (Interpretation 2) with some modification (see explanation in text). Sources of ages for diatom events: 1 = Koizumi and Tanimura (1985); 2 = Koizumi (1992); 3 = Barron (1992); and 4 = Gersonde and Burckle (1990). See Table 1 caption for further explanation; # = isolated, possibly local, occurrence.

sistent, but typically few, neritic planktonic diatoms typical of the Arcto-Boreal region (Koizumi, 1973; Sancetta and Silvestri, 1986) as well as benthic diatoms displaced from shelf environments. These taxa include *Thalassiosira gravida*, *Porosira glacialis*, *Detonula conferavae*, *Thalassiosira insigna*, *Thalassiosira hyalina*, *Pyxidicula zabelinae*, *Delphineis* spp., *Odontella aurita*, *Actinopytchus senarius*, *Paralia sulcata*, and *Pseudopyxilla americana* as well as representatives of the benthic genera *Cocconeis* and *Diploneis*; they are taken as evidence for sediment transport from the Bering Sea or Aleutian Shelf. It should be noted that this distinct arcto-boreal diatom assemblage only evolved in the latest Miocene (Barron, 1980a; Oreshkina, 1985), so that such a Bering Sea or Aleutian influence on sedimentation may extend further back in time (see Gladenkov and Barron, this volume). This transport must have been contemporaneous, because reworked diatoms are extremely rare in the middle Miocene through Pleistocene of Site 884. Sparse occurrences of late Miocene to early Pliocene diatoms and early Miocene diatoms are present in selected intervals of the upper Pliocene and Pleistocene sediments.

### Site 882

A complete sequence of diatom zones from late Miocene Subzone a of the *Neodenticula kamtschatica* Zone through the late Quaternary *Neodenticula seminae* Zone was cored at Site 882 on the top of the Detroit Seamount at 50°21.8'N; 167°36.0'E (water depth, 3255 m) (Fig. 5). The two holes that were drilled penetrated a 398-m-thick section consisting of diatom oozes with intervals of clayey diatom

oozes down to approximately 70 mbsf. Below this level, occasional intervals of diatom oozes with calcite overlay the diatom ooze. Diatoms are generally abundant to common and well preserved to moderately well preserved throughout the sequence, and the assemblages are dominated by subarctic, planktonic taxa (*Neodenticula* spp., *Coscinodiscus marginatus*, etc.). Recognition of diatom datum levels was generally straightforward (Table 3), and good agreement was found between the stratigraphic position of datum levels between Holes 882A and 882B. Diatom zonal and subzonal assignments were made using the adopted criteria.

The magnetostratigraphy at Site 882 (Shipboard Scientific Party, 1993b; R. Tiedemann and R. Weeks, pers. comm., 1992) extends down through the Gilbert Chron (Fig. 5); however, the separate events of the Gauss Chron and the upper normal event of the Gilbert Chron are only tentatively identified. The absolute ages of Pliocene and Pleistocene diatom datum levels that are estimated at Site 882 based on the magnetostratigraphy are shown in parentheses on Table 3 and are discussed later.

A surprising result of drilling at Site 882 was the recovery of an anomalously thick lower Pliocene section assignable to Subzones b to c of the *Neodenticula kamtschatica* Zone. Over 190 m of section (Cores 145–882A-20H through -39H), about 180–370 mbsf, were cored throughout this interval (Fig. 4). The diatom assemblages are dominated by *N. kamtschatica* and *Coscinodiscus marginatus*, which are typical of early Pliocene assemblages of the subarctic North Pacific. *Chaetoceros* spores, which are indicative of high continental marginal productivity (Sancetta and Silvestri, 1986), are not espe-

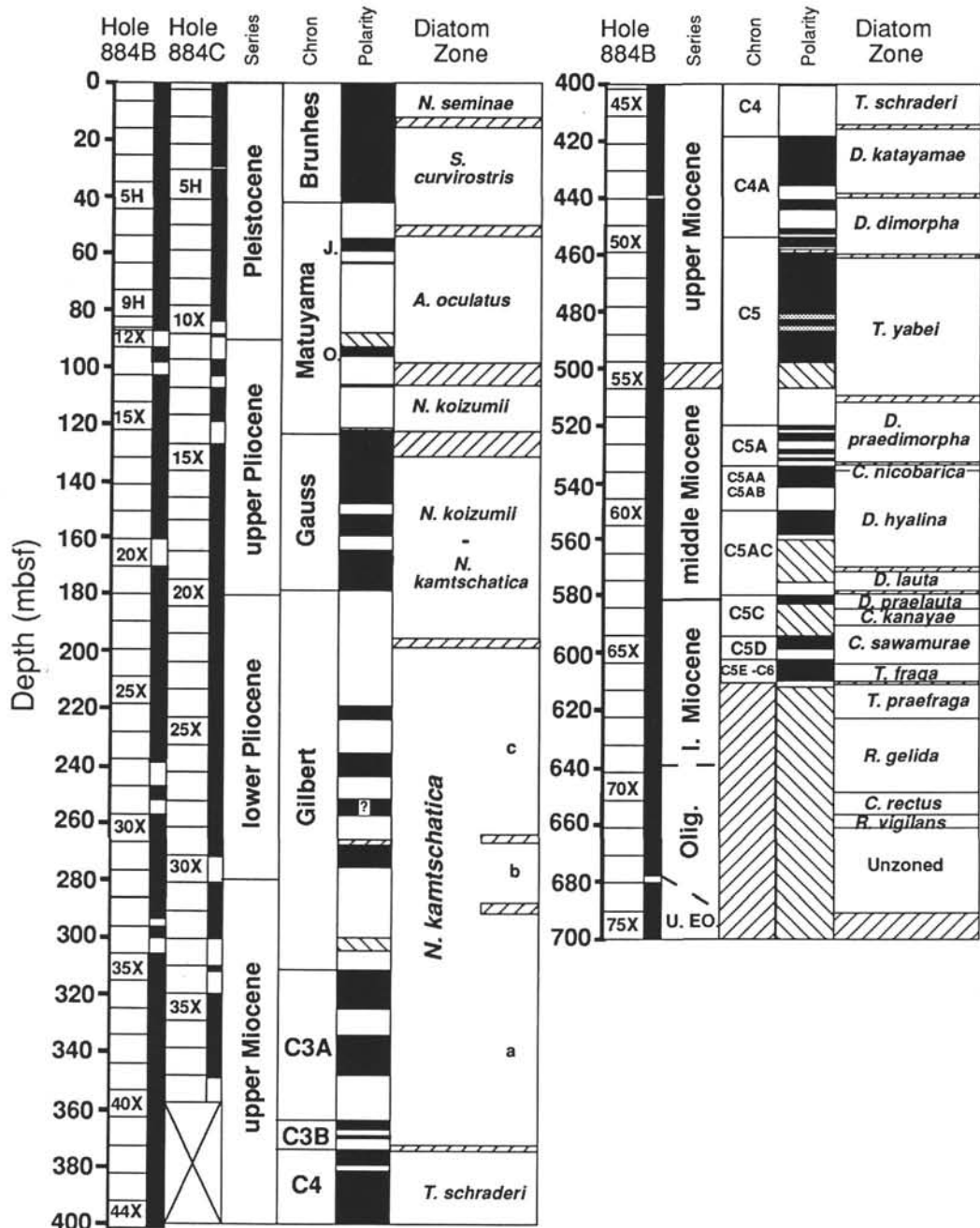


Figure 4. Stratigraphic position of cores, recovery (black), ages, placement of magnetostratigraphic chronos and subchrons, polarity log, and placement of diatom zones in Holes 884B and 884C. The magnetostratigraphy shown is that of Shipboard Scientific Party (1993d) with minor modification (see text). Intervals filled by slanted lines indicate uncertainty in the placement of biostratigraphic boundaries and/or absence of paleomagnetic stratigraphy. J = Jaramillo event, and O = Olduvai event of the Matuyama Chron.

cially abundant in this interval; however, the high numbers of *Thalassiothrix longissima* that are found throughout may be an indicate high oceanic productivity (J. Baldauf, pers. comm., 1992). Relatively consistent and occasionally common occurrences of *Thalassiosira cf. oestrupii* and *Thalassionema nitzschiooides* indicate incursions of transitional waters that are associated with the subarctic polar front. Sparse occurrences of subtropical taxa such as *Hemidiscus cuneiformis* and *Azpeitia nodulifera* suggest relatively warmer conditions.

### Site 883

Site 883 was also drilled on the top of Detroit Seamount ( $51^{\circ}11.9'N$ ,  $167^{\circ}46.1'E$ ; water depth, 2396 m), 49 nmi to the north of Site 882.

Diatoms generally are abundant to common and well preserved to moderately well preserved throughout the lower Miocene through Quaternary section cored above 655 mbsf at Site 883; however, almost no diatoms were observed in the Paleogene section. With the exception of the middle Miocene *Thalassiosira yabei* and *Crucidenticula nicobarica* Zones, all of the Neogene North Pacific diatom zones can be recognized from the early Miocene *Thalassiosira praefraga* Zone through the late Pleistocene *Neodenticula seminae* Zone (Fig. 6). Standard diatom datum levels have been used to recognize these zones (Table 4), and little or no displacement of diatom biostratigraphic horizons is apparent among Holes 883B, 883C, and 883E.

The magnetostratigraphy at Site 883 extends down to the third normal event of the Gilbert reversed polarity Chron (Shipboard Sci-

entific Party, 1993c; G. Dubuisson, pers. comm., 1993) (Fig. 6). The absolute ages of Pliocene to Pleistocene diatom datum levels that are estimated at Site 883 based on the magnetostratigraphy are shown in parentheses on Table 4 are discussed later.

A possible unconformity or compressed interval at the Pliocene/Pleistocene boundary is suggested by the coincidence of the FO of *Simonseniella curvirostris* (1.58 Ma) and the last common occurrence (LCO) of *Neodenticula koizumii* (2.0 Ma) in the interval between Samples 145-883B-6H-CC and -7H-CC (55.4 to 64.9 mbsf) in Hole 883B and between Samples 145-883C-7H-CC and -883C-8H-CC (60.0-69.5 mbsf) in Hole 883C (Table 4). Paleomagnetic stratigraphy, however, identifies the Olduvai event of the Matuyama Chron (1.98–1.76 Ma) at about 67 to 70 mbsf in Hole 883B, suggesting that the LO of *N. koizumii* may be younger at Site 883 than it is at Sites 882 and 881.

At Site 882, the early Pliocene was characterized by high sedimentation rates (ca. 115 m/m.y.) that began near the Miocene/Pliocene boundary (5.1 Ma) and apparently ended at about 3.4 Ma (Table 3). A correlative lower Pliocene interval occurs between ca. 170 and 320 mbsf in Holes 883B and 883C (Fig. 6) and is also characterized by high (ca. 100 m/m.y.) sediment accumulation rates.

The LCO of *Thalassionema schraderi* (7.45–7.35 Ma) in Sample 145-883B-46X-CC (438.9 mbsf) is anomalous in Hole 883B because it falls above normally younger datum levels: the FO of *Thalassiosira jacksonii* (6.6–6.5 Ma) in Sample 145-883B-46X-CC, the FO of *Neodenticula kamtschatica* (7.2–7.1 Ma) in Sample 145-883B-49X-CC; and the first occurrence of *Nitzschia reinholdii* (7.3–7.2 Ma) in Sample 145-883B-50X-CC. Reworking of *T. schraderi* seems likely in Hole 883B.

The entire late middle Miocene, as well as the earliest late Miocene (ca. 13.1–9.8 Ma), is compressed within or removed from the interval between Sample 145-883B-59X-2, 22–23 cm (558.72 mbsf), and the base of Core 145-883B-57X (547.1 mbsf). Within this interval, Sample 145-883B-58X-CC does contain a *Denticulopsis praedimorpha* Zone assemblage (12.8–11.4 Ma), but unfortunately only 0.83 m was recovered in Core 145-883B-58X. An attempt to recover this compressed interval in Core 145-883E-1R (547.0–556.5 mbsf) failed because the top of the 6.15-m-thick section recovered in that core correlates with the *Denticulopsis hyalina* Zone and is older than 13.1 Ma.

Thus, either a greatly compressed interval or two hiatuses—one removing the *Thalassiosira yabei* Zone (11.4–9.8 Ma) and the other removing the *Crucidenticula nicobarica* Zone (13.1–12.8 Ma)—must be present at Site 883. An equivalent interval also is missing or greatly compressed at Gulf of Alaska DSDP Site 183 (Barron, 1989).

Sample 145-883B-68X-CC, 3–4 cm, is assigned to the early Miocene *Thalassiosira praefraga* Zone based on the presence of *Azpeitia oligocenica* and *Cavittatus rectus* and the absence of *Thalassiosira fraga* and *Rocella* spp. (see Gladenkov and Barron, this volume). Below, at the base of the core catcher (interval ca. 39 cm), a poorly preserved latest Oligocene(?) assemblage containing *Lisitzinia ornata*, *Cavittatus jouseanus*, and *Kieseleviella magnaareolata* was observed. A sharp lithologic break between greenish gray, diatom-rich calcareous chalk above and light brownish gray, diatom-poor calcareous chalk below the 10-cm level in the core catcher of Core 145-883B-68X possibly represents an unconformity between the late Oligocene (>24 Ma) and the latest part of the early Miocene *T. praefraga* Zone (ca. 20.5 Ma).

### Site 881

An apparently continuous sequence of upper Miocene through Quaternary sediments was recovered at Site 881 (47°6.1'N, 161°29.5'E; water depth, 5531 m). The 335-m-thick section consists of diatom ooze overlain by clayey diatom ooze, the latter containing numerous ash layers. Diatoms generally are common to abundant and moderately well preserved to well preserved throughout the section recovered at Site 881. In parts of the upper Pliocene and Pleistocene section, how-

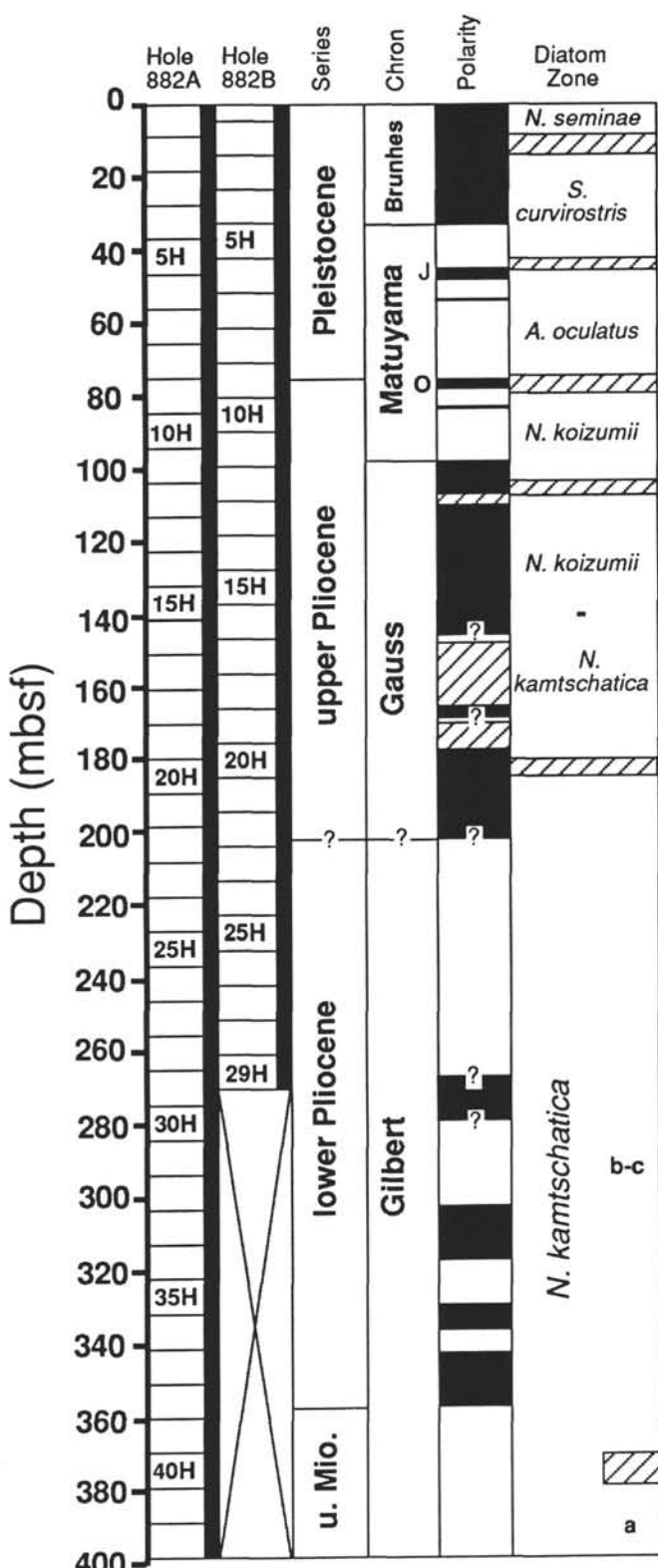


Figure 5. Stratigraphic position of cores, recovery (black), ages, placement of magnetostratigraphic chronos and subchrons, and placement of diatom zones in Holes 882A and 882B. The magnetostratigraphy shown is that of Shipboard Scientific Party (1993b) and R. Tiedemann and R. Weeks (pers. comm., 1992). Intervals filled by slanted lines indicate uncertainty in the placement of biostratigraphic boundaries.

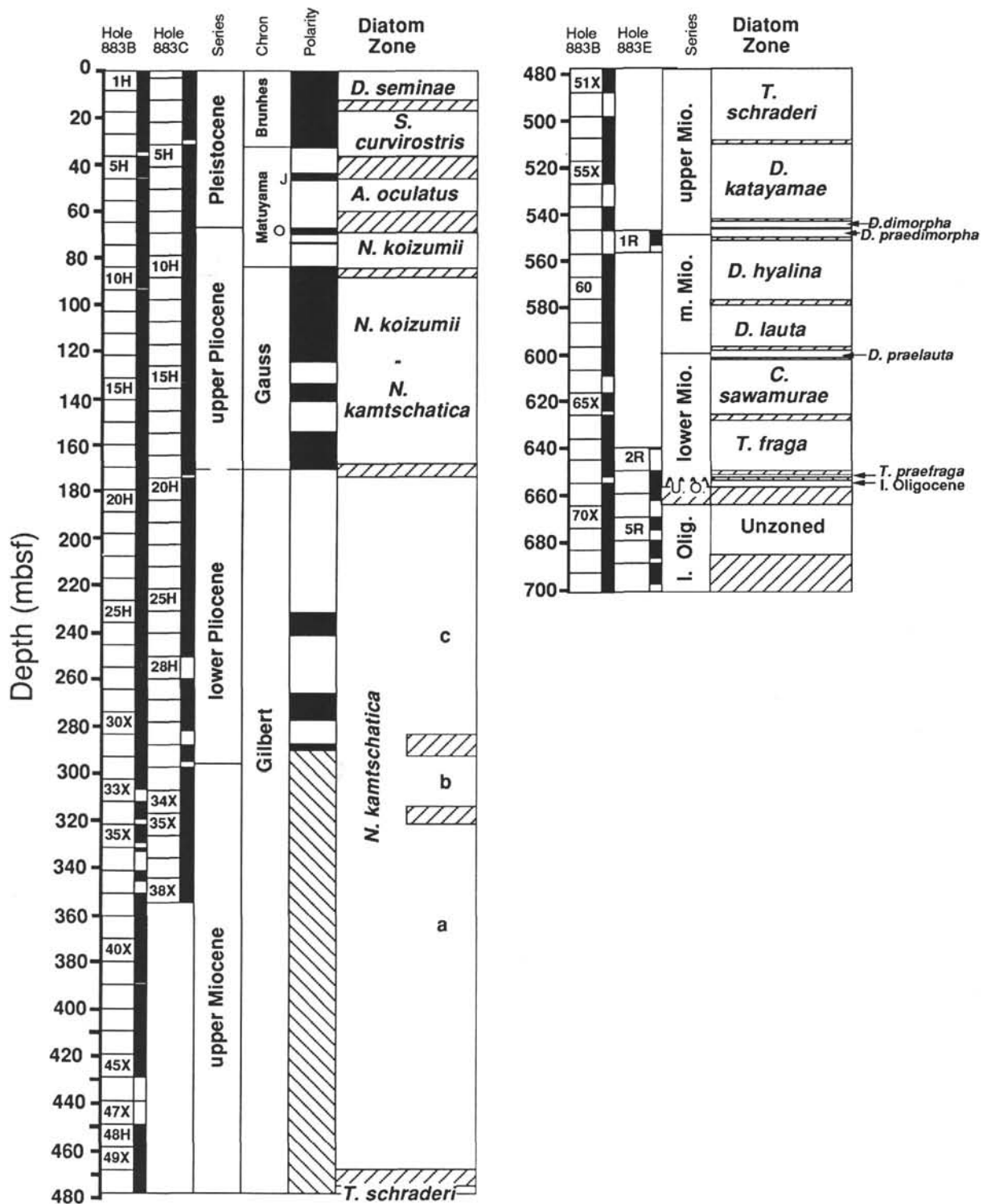


Figure 6. Stratigraphic position of cores, recovery (black), ages, placement of magnetostratigraphic chronos and subchrons, polarity log, and placement of diatom zones in Holes 883B, 883C, and 883E. The magnetostratigraphy shown is that of Shipboard Scientific Party (1993c) and G. Dubuisson (pers. comm., 1993). Intervals filled by slanted lines indicate uncertainty in the placement of biostratigraphic boundaries and/or absence of paleomagnetic stratigraphy. U.O. = upper Oligocene.

ever, diatoms are few in abundance because of increases in clay and other detrital materials. Assemblages commonly are dominated by *Coscinodiscus marginatus*, a large, robust diatom that is resistant to dissolution and fragmentation.

A complete sequence from the late Miocene *Thalassionema schraderi* Zone through the late Quaternary *Neodenticula seminae*

Zone was recovered from the four holes cored at Site 881 (Fig. 7). Hole 881A, represented by a single core, recovered only uppermost Quaternary sediments. An uppermost Pliocene through Quaternary record (the last 2.6 m.y.) was recovered in Holes 881B and 881C. Hole 881D was drilled to retrieve uppermost lower Pliocene and lowermost upper Pliocene not recovered in Hole 881C. Hole 881C

**Table 3.** Age and stratigraphic position of diatom datum levels and magnetic polarity events in Holes 882A and 882B.

Datum	Age (Ma)	Source	Hole 882A		Hole 882B	
			Interval	Depth (mbsf)	Interval	Depth (mbsf)
LO <i>Simonsenella curvirostris</i>	0.3	2	1H-CC/2H-CC	8.8/18.3	1H-CC/2H-CC	4.4/13.9
B C1n.1n	0.78		4H-4, 120 cm	33.5	5H-1, 40 cm	33.3
T C1r.1n	0.98		5H-6, 0-52 cm	44.8-45.32	6H-2, 80 cm	44.7
LCO <i>Actinocyclus oculus</i>	1.0	1	4H-CC/5H-CC	37.3/46.8	5H-CC/6H-CC	42.4/51.9
B C1r.1n	1.05		6H-2, 10 cm	48.4		
FO <i>Simonsenella curvirostris</i>	1.58	1	7H-CC/8H-CC	65.8/75.3	8H-CC/9H-CC	70.9/80.4
LO <i>Pyxidicula horridus</i>	(1.6-1.8)		7H-CC/8H-CC	65.8/75.8	9H-CC/10H-CC	80.4/89.9
T C2n.1n	1.76		9H-1, 10 cm	75.4		
B C2n.1n	1.98		9H-2, 135 cm	78.15		
LO <i>Neodenticula koizumii</i>	(2.0-2.1)		8H-CC/9H-CC	75.3/84.8	9H-CC/10H-CC	80.4/89.9
T C2An.1n	2.6		11H-3, 80 cm	98.1		
LCO <i>Neodenticula kamtschatica</i>	2.63-2.7	1	11H-CC/12H-CC	103.8/113.3	11H-CC/12H-CC	99.4/108.9
FO <i>Neodenticula seminae</i>	2.7	1	11H-CC/12H-CC	103.8/113.3	11H-CC/12H-CC	99.4/108.9
B C2An.1n?	3.054			146.5		
LO <i>Thalassiosira marujamica</i>	(3.1-3.2)		16H-CC/17H-CC	151.3/160.8	17H-CC/18H-CC	156.4/165.9
B C2An.2n?	3.221			165.5		
LO <i>Thalassiosira jacksonii</i>	(3.3-3.4)		18H-CC/19H-CC	170.3/179.8		
FO <i>Neodenticula koizumii</i>	(3.4)		19H-CC/20H-CC	179.8/189.3	19H-CC/20H-CC	175.4/184.9
B C2An.3n?	3.553			202.0		
FO <i>Actinocyclus oculus</i>	(3.6-3.7)		21H-CC/22H-CC	198.8/208.3	20H-CC/21H-CC	184.9/194.4
T C3n.1n?	4.033			267.0		
B C3n.1n?	4.134			279.0		
T C3n.2n	4.265			302.0		
B C3n.2n	4.611			317.0		
LO <i>Thalassiosira jacksonii</i> (plicate)	(4.5-4.6)		34H-CC/35H-CC	322.3/331.8		
T C3n.3n	4.694			329.0		
B C3n.3n	4.611			336.0		
T C3n.4n	4.812			342.0		
FO <i>Thalassiosira latimarginata</i> s.str.	(4.8-4.9)		36H-CC/37H-CC	341.3/350.8		
B Cn.4n	5.046			357.0		
FO <i>Thalassiosira jacksonii</i> (plicate)	(4.9-5.1)		37H-CC/38H-CC	350.8/360.3		
FO <i>Thalassiosira latimarginata</i> s.ampl.	(4.9-5.1)		37H-CC/38H-CC	350.8/360.3		
FO <i>Thalassiosira oestrupii</i>	5.4	3	39H-CC/40H-CC	369.8/379.3		
LO <i>Thalassiosira miocenica</i>	5.7	1	40H-CC/41H-CC	379.3/388.8		
FO <i>Thalassiosira miocenica</i>	6.2	3	>42H-CC	>398.8		

Notes: Magnetic polarity events after Shipboard Scientific Party (1993b) and R. Tiedemann and R. Weeks (written comm., 1992). Sources of ages for diatom events: 1 = Koizumi and Tanimura (1985); 2 = Koizumi (1992); and 3 = magnetostratigraphic correlations of Sites 884 and 887 (Tables 1 and 2). See Table 1 caption for further explanation.

penetrated the oldest sediments at this site, which are late Miocene (ca. 7.4 Ma) in age. The stratigraphic position of diatom datum levels in Holes 881B and 881C are listed in Table 5.

The magnetostratigraphy at Site 881 extends down to the uppermost part of the Gilbert Chron (Shipboard Scientific Party, 1993a). The absolute ages of Pliocene to Pleistocene diatom datum levels that are estimated at Site 881 based on the magnetostratigraphy are shown in parentheses on Table 5 and are discussed below.

## DISCUSSION

The age estimates of the Miocene and Pliocene diatom datum levels derived from the magnetostratigraphy at Sites 881-884 and 887 allow comparison to previously published age estimates (Tables 6, 7). The present age estimates are derived from correlation to the Cande and Kent (1992) geomagnetic polarity time scale; however, differing sample spacing and sediment accumulation rates at the various sites result in varying degrees of refinement in the estimated ages. Thus, resolution of the degree of isochroneity or diachroneity of individual diatom datum levels in the North Pacific is limited. Nevertheless, a number of observations can be made.

### Miocene Datum Levels

Based on available magnetostratigraphic control (Table 6) and synthesis studies (Koizumi, 1985; Akiba, 1986; Barron, 1992), the following Miocene datum levels appear to be essentially isochronous and widely applicable in the North Pacific: the FO of *C. kanayae* (16.9 Ma), the FO of *Denticulopsis praelauta* (16.3 Ma), the FO of *D. lauta* (15.9 Ma), the FO of *D. hyalina* (14.9 Ma), first common occurrence (FCO) of *D. hustedtii* (13.1 Ma), the FO of *D. praedimorpha* (12.8 Ma), the LCO of *D. praedimorpha* (11.4 Ma), FO of *D. dimorpha* (9.8 Ma), FO of *Thalassionema schraderi* (9.3 Ma), the LO of *D. dimorpha* (9.0 Ma), the LCO of *D. hustedtii* (8.4 Ma), the LCO of *T. schraderi* (7.45-7.35 Ma), the FO of *Neodenticula kamtschatica*

(7.2-7.1 Ma), the LO of *Cavitatus jouseanus* (6.5-6.6 Ma), the FO of *Thalassiosira miocenica* (6.2 Ma), the FO of *T. praeoestrupii* (5.95 Ma), the LO of *Rouxia californica* (5.7-5.75 Ma), and the FO of *T. oestrupii* (5.3 Ma). The FO of *Crudenticula sawamuriae* (18.4 Ma) is isochronous between Sites 884 and 887, but it is younger in the equatorial Pacific (17.55 Ma). Similarly, the FO of *Thalassiosira fraga* (20.3 Ma) may also be widely isochronous, but its magnetostratigraphic calibration is more equivocal. Not surprisingly, virtually all of these datum levels have been widely used in various North Pacific diatom zonations (Koizumi, 1973, 1985; Barron, 1980a, 1981, 1985b, 1992; Maruyama, 1984; Koizumi and Tanimura, 1985; Akiba, 1986). It should be pointed out, however, that the FO of *N. kamtschatica* is delayed in the California region (ca. 5.3 Ma), whereas *Rouxia californica* has an earlier LO (about 6.5 Ma) according to Barron (1992).

The FO of *Actinocyclus ingens* var. *nodus* (15.8 Ma) and the FO of *Simonsenella barboi* (12.4 Ma) may be approximately isochronous between Sites 884 and 887. However, comparison with other datum levels (Barron, 1992) suggests that these two cold-water diatoms may have delayed FOs in the California region (40°-33°N) (15.1 and 11.5 Ma, respectively).

Likewise, the FOs and LOs of certain warm-water diatom taxa appear to vary across latitude in the North Pacific—namely, the LO of *Crudenticula nicobarica* (12.8-12.4 Ma), the FO of *Hemidiscus cuneiformis* (11.7-10.4 Ma), the FO of *Nitzschia fossilis* (8.4-7.6 Ma), and the FO of *N. reinholdii* (7.2-6.9 Ma)—but confirmation of this diachroneity must await magnetostratigraphic studies at lower latitudes (45°-30° N) in the North Pacific. The LO of *Thalassiosira miocenica*, another tropical diatom, appears to be slightly diachronous (5.9-5.7 Ma) in the North Pacific.

### Pliocene Datum Levels

The FO of *Thalassiosira jacksonii* (plicate form) (5.0 Ma), the FO of *T. latimarginata* s. str. (4.9 Ma), the LO of *T. jacksonii* (plicate form) (4.6 Ma), and the LO of *T. marujamica* (3.2-3.1 Ma) appear to

**Table 4.** Age and stratigraphic position of diatom datum levels and magnetic polarity events in Holes 883B and 883C.

Datum	Age (Ma)	Source	Hole 883B		Hole 883C	
			Interval	Depth (mbsf)	Interval	Depth (mbsf)
LO <i>Simonsenella curvirostris</i>	0.3	2	1H-CC/2H-CC	7.9/17.4	2H-CC/3H-CC	12.5/22.0
B C1n.1n	0.78		4H-5, 50 cm	33.30	5H-3, 55 cm	35.05
T C1r.1n	0.984		5H-5, 120 cm	43.50	6H-1, 85–125 cm	41.85–42.25
LCO <i>Actinocyclus oculatus</i>	1.0	1	4H-CC/5H-CC	36.4/45.9	5H-CC/6H-CC	41.0/50.5
B C1r.1n	1.049		6H-1, 100 cm	47.00	6H-5, 135 cm	48.35
FO <i>Simonsenella curvirostris</i>	1.58	1	6H-CC/7H-CC	55.4/64.9	7H-CC/8H-CC	60.0/69.5
LO <i>Pxydicula horridus</i>	(1.6–1.8)		6H-CC/7H-CC	55.4/64.9	7H-CC/8H-CC	60.0/69.5
T C2n.1n	1.757		8H-2, 70 cm	67.1	8H-5, 150 cm	67.5
LO <i>Pxydicula pustulata</i>	(1.9–2.1)		7H-CC/8H-CC	64.9/74.4	7H-CC/8H-CC	60.0/69.5
LO <i>Neodenticula koizumii</i>	(1.6–1.8)		6H-CC/7H-CC	55.4/64.9	7H-CC/8H-CC	60.0/69.5
B C2n.1n	1.983		8H-4, 60 cm	70	8H-7 to 9H-2	69.70–71.05
T C2An.1n	2.6		9H-7 to 10H-1	83.7–84.3	10H-4, 50 cm	84.00
LCO <i>Neodenticula kamtschatica</i>	2.63–2.7	1	9H-CC/10H-CC	83.9/93.4	9H-CC/10H-CC	79.9/88.5
FO <i>Neodenticula seminae</i>	2.7	1	9H-CC/10H-CC	83.9/93.4	9H-CC/10H-CC	79.9/88.5
B C2An.1n	3.054			125.15		
T C2An.2n	3.127			133.9		
LO <i>Thalassiosira marujamica</i>	(3.1)		15H-2, 91 cm/15H-2, 135 cm	133.8/134.25	15H-CC/16H-CC	136.0/145.5
LO <i>Thalassiosira jacksonii</i>	(3.1–3.2)		14H-CC/15H-CC	131.4/140.4	15H-CC/16H-CC	136.0/145.5
B C2An.2n	3.221			141.45		
T C2An.3n	3.325			154.9		
FO <i>Neodenticula koizumii</i>	(3.45–3.55)		18H-CC/19H-CC	159.9/168.4	18H-CC/19H-CC	164.5/174.0
B C2An.3n	3.553			170.4		
FO <i>Actinocyclus oculatus</i>	(3.7)		20H-CC/21H-CC	178.9/188.4	20H-CC/21H-CC	183.5/193.0
T C3n.1n	4.033			231.65		
B C3n.1n	4.134			241.45		
T C3n.2n?	4.265			266.2		
B C3n.2n?	4.432			277.95		
T C3n.3n	4.611			287.45		
LO <i>Thalassiosira jacksonii</i> (plicate)	(4.5–4.6)		30H-CC/31H-CC	283.4/292.9	30X-CC/31X-CC	278.3/288.0
LO <i>Thalassiosira insignia</i>	(4.5–4.7)		30H-CC/31H-CC	283.4/292.9		
FO <i>Thalassiosira latimarginata</i>	(4.8–4.9)		31H-CC/32X-CC	292.9/302.5	31X-CC/32X-CC	288.0/297.6
FO <i>Thalassiosira jacksonii</i> (plicate)	(5.3–5.4)		33X-CC/34X-CC	312.2/321.9	34X-CC/35H-CC	314.19/326.5
FO <i>Thalassiosira oestrupii</i>	5.3	3	33X-CC/34X-CC	312.2/321.9	34X-CC/35H-CC	314.19/326.5
LO <i>Thalassiosira miocenica</i>	5.7	1	34X-CC/35X-CC	321.9/331.5	35H-CC/36H-CC	326.5/336.0
FO <i>Thalassiosira praeoestrupii</i>	5.95	4	34X-CC/35X-CC	321.9/331.5		
LO <i>Thalassiosira praecoxysa</i>	6.3	5	39X-CC/40X-CC	370.2/380.0		
FO <i>Thalassiosira miocenica</i>	6.2	3	44X-CC/45X-CC	419.2/429.0		
FO <i>Thalassiosira jacksonii</i>	6.5–6.6	3	46X-CC/47X-CC	439.3/448.7		
FO <i>Neodenticula kamtschatica</i>	7.1–7.2	3	49X-CC/50X-CC	468.1/477.9		
FO <i>Nitzschia reinholdii</i>	7.2–7.3	3	50X-CC/51X-CC	477.9/487.9		
LO <i>Thalassionema schraderi</i>	7.4	3	45X-CC/46X-CC	429.0/438.9		
FO <i>Nitzschia fossilis</i>	7.6–7.7	3	53X-CC/54X-CC	507.6/517.4		
LCO <i>Denticulopsis hustedtii</i>	8.4	3	53X-CC/54.2, 104 cm	507.6/510.14		
LO <i>Denticulopsis dimorpha</i>	9.0	3	57.4, 104 cm/57X-CC	542.6/547.1		
FO <i>Denticulopsis dimorpha</i>	9.8	3	57X-CC/58X-CC	547.1/557.0		
FO <i>Denticulopsis praedimorpha</i>	12.8	3	58X-CC/59.2, 22 cm	557.0/558.72		
FCO <i>Denticulopsis hustedtii</i>	13.1	3	58X-CC/59.2, 22 cm	557.0/558.72		
FO <i>Denticulopsis hyalina</i>	15.1	3	60X-CC/61.2, 104 cm	577.0/579.54		
FO <i>Denticulopsis lauta</i>	15.9	3	62X-CC/63.2, 104 cm	597.0/599.54		
FO <i>Denticulopsis praelauta</i>	16.3	3	63.2, 104 cm/63.4, 104 cm	599.54/602.54		
FO <i>Crucidenticula sawamuriae</i>	18.4	3	65X-CC/66.2, 104 cm	626.3/628.84		
LO <i>Apektia oligocenica</i>	20.3	5	67X-CC/68X-CC, 3	645.1/652.13		
FO <i>Thalassiosira fraga</i>	20.1	5	68.4, 22 cm/68X-CC, 3	649.8/652.13		
O <i>Lisitzinia ornata</i>	24.3–27.9	6	68X-CC	654.8		
LO <i>Pixilla gracilis</i>	30.3	6	68X-CC/69X-CC	654.8/664.4		
FO <i>Cavatulus miocenica</i>	30.6	6	69X-CC/70X-CC	664.4/674.1		

Notes: Magnetic polarity events after Shipboard Scientific Party (1993c) and G. Dubuisson (written comm., 1993). Sources of ages of diatom events: 1 = Koizumi and Tanimura (1985); 2 = Koizumi (1992); 3 = magnetostratigraphic correlations of Sites 884 and 887 (Tables 1 and 2); 4 = Boden (1993); 5 = Barron (1992); and 6 = Harwood and Maruyama (1992). See Table 1 caption for further explanation.

be nearly isochronous in the North Pacific region of Leg 145 (Table 7); however, Koizumi (1992) records older ages for the FO of *T. latimarginata* (as *T. trifulta*) (to 5.7 Ma) and the LO of *T. marujamica* (5.4 Ma) from the Sea of Japan. It also should be pointed out that *T. marujamica* can be very sparse and sporadic in Leg 145 sediments (Barron, this volume), so that recognition of its LO may be very difficult.

The LO of *Thalassiosira insignia* (ca. 4.7 Ma) also may appear to be approximately isochronous in the North Pacific (see Barron, 1980a). However, *T. insignia* is very sparse and sporadic in Leg 145 sediments, and probably is more common in neritic regions of the North Pacific and the Bering Sea (Barron, 1980a; J.A. Barron, unpubl. data).

As recognized by Koizumi and Tanimura (1985), the FO of *Neodenticula koizumii* is diachronous across latitude, ranging from about 3.95–3.75 Ma at Site 881 to 3.4 Ma at Site 882. All of these occurrences are younger than the 4.2 Ma (Subchron C3r.1r) age for the FO of *N. koizumii* reported by Basilian et al. (1991) in Kamchatka, and one must regret the widespread use of this datum level in North Pacific diatom stratigraphy where it marks the top of the *Neoden-*

*ticula kamtschatica* Zone and the base of the overlying *Neodenticula koizumii*–*N. kamtschatica* Zone (Fig. 2).

We hoped that the FO of *Actinocyclus oculatus* might prove to be a more reliable stratigraphic marker than the FO of *Neodenticula koizumii* in the middle part of the Pliocene north of about 40°N. Valves of *A. oculatus* are easier to identify at low magnification in the light microscope because of their commonly blue interference colors and distinctive areolar pattern. Similarly, the more robust nature of the valves of *A. oculatus*, compared with those of *N. koizumii*, would suggest that it should be less susceptible to dissolution. The magnetostratigraphy, however, indicates that the FO of *A. oculatus* varies from about 3.9 to 3.65 Ma at the Leg 145 sites (Table 7).

Similarly, the LO of *Thalassiosira jacksonii* also shows a considerable range in Leg 145 sediments (ca. 3.7–3.1 Ma), which supports Koizumi's (1992) data from the Sea of Japan. This diachroneity probably reflects the sparse occurrence of *T. jacksonii* in Leg 145 sediments (Barron, this volume) as well as the relatively delicate nature of its valves.

Table 5. Age and stratigraphic position of diatom datum levels and magnetic polarity events in Holes 881B, 881C, and 881D.

Datum	Age (Ma)	Source	Hole 881B		Hole 881C	
			Interval	Depth (mbsf)	Interval	Depth (mbsf)
LO <i>Simonsenella curvirostris</i>	0.30	2	3H-CC/4H-CC	24.5/34.0	3H-CC/4H-CC	22.8/32.3
B C1n.In	0.78		6H-3, 0 cm	46.5	6H-5, 30 cm	48.1
T C1r.In	0.984		7H-2, 55 cm/7H-4, 60 cm	55.05–58.1	7H-5, 30 cm	57.6
LO <i>Rhizosolenia matuyamai</i>	0.91–1.04	1	7H-6, 120 cm	61.7	7H-CC/8H-CC	60.8/70.3
B C1r.1r	1.049				8H-2, 20 cm or 8H-4, 140 cm	62.5 or 66.7
FO <i>Rhizosolenia matuyamai</i>	0.98–1.12	1	7H-CC/8H-CC	62.5/72.0	8H-CC/9H-CC	70.3/79.8
LCO <i>Actinocyclus oculatus</i>	1.0	1	10H-CC/11H-CC	91.0/100.5	7H-CC/8H-CC	60.8/70.3
FO <i>Simonsenella curvirostris</i>	1.58	1	10H-CC/11H-CC	91.0/100.5	11H-CC/12H-CC	98.8/108.3
LO <i>Pyxidicula pustulata</i>	(1.7)		12H-3, 10 cm	103.6	11H-CC/12H-CC	98.8/108.3
T C2n.In	1.757		12H-6, 95 cm	108.95	12H-5, 20 cm?	105?
B C2n.In	1.983		12H-6, 95 cm	108.95	13H-2, 10 cm?	109.9?
LO <i>Neodenticula koizumii</i>	2.0	2	11H-CC/12H-CC	100.5/110.0	11H-CC/12H-CC	98.9/108.3
T C2n.2n	2.197		13H-6, 30 cm	117.8/119.8	14H-4, 75 cm	123.05
B C2n.2n	2.229		14H-2, 50 cm?	121.5?	14H-7, 70 cm	127.5
LO <i>Thalassiosira convexa</i>	2.4	1	15H-CC/16H-CC?	138.5/148.0		
T C2An.In	2.6		18H-2, 130 cm	164.8		
Hole 881D						
T C2An.In	2.6		1H-6, 5 cm/2H-1, 0 cm	163.0/164.5		
LCO <i>Neodenticula kamtschatica</i>	2.63–2.7	1	1H-CC/2H-CC	164.75/174.0	18X-CC/21-1, 25 cm	162.3/182.0
FO <i>Neodenticula seminae</i>	2.7		1H-CC/2H-CC	164.75/174.0	18X-CC/21-1, 25 cm	162.3/182.0
B C2An.In	3.054	1	3H-3, 120 cm	178.2		
LO <i>Thalassiosira jacksonii</i>	(3.1)		3H-4, 125 cm/3H-5, 125 cm	179.75/181.25	18X-CC/21-1, 25 cm	162.3/182.0
T C2An.2n	3.127		3H-5, 150 cm	181.5		
LO <i>Thalassiosira marujamica</i>	(3.1–3.2)		3H-5, 125 cm/3H-CC	181.25/183.5	18X-CC/21-1, 25 cm	162.3/182.0
B C2An.2n	3.221		4H-1, 70 cm	184.2		
T C2An.3n	3.325		4H-2, 120 cm	186.2		
B C2An.3n	3.553		5H-4, 40 cm/5H-6, 100 cm	197.9/201.5		
T C3n.In	4.033		6H-6, 80 cm?	210.8		
FO <i>Neodenticula koizumii</i>	(3.75–3.95)		>6H-CC	>212.0		
FO <i>Actinocyclus oculatus</i>	(3.75–3.95)		>6H-CC	>212.0	23X-CC/25X-CC	209.7/228.7
LO <i>Thalassiosira jacksonii</i> (plicate)	4.6	3			23X-CC/25X-CC	209.7/228.7
FO <i>Thalassiosira latimarginata</i>	4.8–4.9	3			27X-CC/29X-CC	248.0/267.2
FO <i>Thalassiosira oestrupii</i>	5.3	3			29X-CC/30X-CC	267.2/276.9
LCO <i>Rouxia californica</i>	6.3	4			30X-CC/32-1, 46 cm	276.9/286.96
FO <i>Thalassiosira jacksonii</i>	6.5–6.6	3			32X-3, 46 cm/32X-CC	288.4/296.20
FO <i>Nitzschia reinholdii</i>	7.2–7.3	3			32X-CC/35X-CC	296.2/325.10
FO <i>Neodenticula kamtschatica</i>	7.1–7.2	3			35X-CC/36X-CC	325.1/334.8
LO <i>Thalassionema schraderi</i>	7.4	3			35X-CC/36X-CC	325.1/334.8

Notes: Magnetic polarity events after Shipboard Scientific Party (1993a). Sources of ages for diatom events: 1 = Koizumi and Tanimura (1985); 2 = Koizumi (1992); 3 = magnetostratigraphic correlations of Sites 884 and 887; and 4 = Barron (1992). See Table 1 caption for further explanation.

Unfortunately, the latest Pliocene datum levels, that is, the LO of *Pyxidicula zabelinae*, the LO of *Neodenticula koizumii*, the LO of *P. horridus*, have only been resolved to within 200 k.y., so little can be said about their isochroneity. Koizumi's (1992) proposal to use the LCO of *N. koizumii* to mark the top of the *N. koizumii* Zone and the base of the overlying *Actinocyclus oculatus* Zone appears to be warranted. Paleomagnetically calibrated ages at Sites 882 and 884 are in good agreement with Koizumi's (1992) 1.9–2.1 Ma age estimates for this datum in the Sea of Japan. The younger age estimate (1.8–1.6 Ma) for this datum at Site 883 is the exception. As noted earlier, however, an unconformity likely truncates the top of the Olduvai event of the Matuyama Chron at Site 883. These data support the arguments of Sancetta and Silvestri (1986) and others, that quantitative studies are necessary to resolve age estimates of the latest Pliocene and Pleistocene diatom datum levels in the North Pacific adequately.

## SUMMARY

Sediments cored during Leg 145 at Sites 881 to 884 and 887 provide valuable lower Miocene through Pleistocene reference sections for North Pacific diatom biostratigraphy. Essentially complete late early Miocene through Quaternary magnetostratigraphies at Sites 884 and 887 allow the first detailed magnetostratigraphic calibration of over 40 diatom datum levels between Subchron C5En (18.817–18.317 Ma) and Subchron C3Bn (6.901–6.744 Ma) in the North Pacific. In addition, the magnetostratigraphic calibrations of 20 younger (latest Miocene and Pliocene) diatom datum levels are provided from Sites 881, 882, 883, 884, and 887.

When compared with each other and with published data, most of those late early Miocene through Pliocene diatom datum levels that have been widely used in the North Pacific for biostratigraphy appear to be isochronous within the level of resolution constrained by sample spacing. Reliable Miocene diatom datum levels in the North Pacific include the FO of *C. kanayae* (16.9 Ma), the FO of *Denticulopsis praelauta* (16.3 Ma), the FO of *D. lauta* (15.9 Ma), the FO of *D. hyalina* (14.9 Ma), the FCO of *D. hustedtii* (13.1 Ma), the FO of *D. praedimorpha* (12.8 Ma), the LCO of *D. praedimorpha* (11.4 Ma), the FO of *D. dimorpha* (9.8 Ma), the FO of *Thalassionema schraderi* (9.3 Ma), the LO of *D. dimorpha* (9.0 Ma), the LCO of *D. hustedtii* (8.4 Ma), the LCO of *T. schraderi* (7.45–7.35 Ma), the FO of *Neodenticula kamtschatica* (7.2–7.1 Ma), the LO of *Cavatatus jouseanus* (6.5–6.6 Ma), the FO of *Thalassiosira miocenica* (6.2 Ma), the FO of *T. praeoestrupii* (5.95 Ma), the LO of *Rouxia californica* (5.7–5.75 Ma), and the FO of *T. oestrupii* (5.3 Ma). Within the Pliocene, the FO of *Thalassiosira jacksonii* (plicate form) (5.0 Ma), the FO of *T. latimarginata* s. str. (4.9 Ma), the LO of *T. jacksonii* (plicate form) (4.6 Ma), and the LO of *T. marujamica* (3.2–3.1 Ma) appear to be reliable datum levels within the North Pacific region covered by Leg 145.

Available magnetostratigraphy suggests that a few widely used Miocene diatom datum levels are diachronous across latitude in the North Pacific: the FO of *Crucidenticula sawamurae* (18.4–17.55 Ma), the FO of *Actinocyclus ingens* var. *nodus* (15.8–15.1 Ma), and the FO of *Simonsenella barboi* (12.4–11.5 Ma). Although the younger calibration for the FO of *C. sawamurae* comes from the equatorial Pacific, that datum level is isochronous between Sites 884 and 887; so the FO of *C. sawamurae* may be a reliable datum level in the middle-to-high latitude North Pacific. Within the Pliocene, diachroneity is documented

**Table 6.** Comparison of ages of late early Miocene to latest Miocene diatom datum levels derived from magnetostratigraphy in Leg 145 holes with published ages.

Datum	Hole 884B	Site 887	Published ages		
			Age (Ma)	PM?	Source
LO <i>Rouxia californica</i>	5.7–5.75		5.7	Yes	1
LO <i>Thalassiosira miocenica</i>	5.8	5.9*	5.7	Yes	1
LO <i>Thalassiosira singularis</i>	5.8		6.5	No	2
FO <i>Thalassiosira praestrupii</i>	5.95		5.95	Yes	7
FO <i>Thalassiosira miocenica</i>	6.2	6.2*	6.3	Yes	2
FO <i>Thalassiosira jacksonii</i>	6.5–6.6		6.8; 6.1–6.8	No	2; 3
LO <i>Cavitätus jouseanus</i>	6.5–6.6	6.6*	6.5	No	2
FO <i>Thalassiosira marujamica</i>	6.8–6.9		6.0–7.5	No	3
FO <i>Neodenticula kamtschatica</i>	7.1–7.2	7.1–7.2*	7	No	2
FO <i>Nitzschia reinholdii</i>		7.2–7.3*	6.9	No	2
LCO <i>Thalassionema schraderi</i>	7.35–7.45	7.4–7.5*	7.2; 7.6	No	2; 3
FO <i>Nitzschia pfiocena</i>	7.6–7.7		7.8; 8.3	No	3; 2
FO <i>Nitzschia fossilis</i>	7.6–7.7		8.4	No	2
FO <i>Nitzschia rolandii</i>	7.8–7.9		7.5; 8.3–8.5	No	2; 3
FO <i>Thalassiosira gravida</i>	7.9–8.0		7.9–8.0	No	2
FO <i>Thalassiosira singularis</i>	7.9–8.0		7.7–7.9	No	2
FO <i>Nitzschia praereinholdii</i>	8.3		11.7–11.8	No	2
LCO <i>Denticulopsis hustedtii</i>	8.4	8.4*	8.6	No	2
LO <i>Denticulopsis dimorpha</i>	9.0	8.8–8.9*	9.1	No	2
FO <i>Thalassiosira minutissima</i>	9.1	9.4*	9.4–9.7	No	2
FO <i>Denticulopsis katayamae</i>	9.1	9.4*	9.3	No	2
FO <i>Thalassionema schraderi</i>	9.3	9.4*	8.4–8.6	No	2
FO <i>Denticulopsis dimorpha</i>	9.8	9.8–9.9*	9.6	No	2
FO <i>Hemidiscus cuneiformis</i>	10.7–10.9	10.4–10.6	11.7	No	2
LO <i>Nitzschia heteropolica</i>	10.7–10.9	10.6–10.8	11.4	No	2
LO <i>Mediaria splendida</i>	10.7–10.9	11.4–11.5	10.2	No	2
LCO <i>Denticulopsis praedimorpha</i>	11.4	11.2–11.4	11.4	Yes(So)	5; 6
FO <i>Simonsenella barboi</i>	12.4	12.0–12.4*	11.5	Yes	2
LO <i>Crucidenticula nicobarica</i>	12.8	12.4–12.6*	12.2; 12.4	Yes(So); No	6; 2
FO <i>Denticulopsis praedimorpha</i>	12.8	12.7–13.1	12.8	Yes(So)	4; 5
FCO <i>Denticulopsis hustedtii</i>	13.1	12.7–13.1	13.65	No	2
FO <i>Nitzschia heteropolica</i>	13.1–13.2	12.4–12.6*	11.9–12.0	No	2
FO <i>Denticulopsis hustedtii</i>	14.4–14.8	13.6–14.6*	14.2	Yes(So)	4
FO <i>Denticulopsis hyalina</i>	14.9	14.9–15.1*	14.9	Yes	2
FO <i>Actinocyclus ingens</i> var. <i>nodus</i>	15.8	15.5–16.7*	15.1	No	2
FO <i>Denticulopsis lauta</i>	15.9		15.9	No	2
LO <i>Crucidenticula kanayae</i>	16.2		14.7	No	2
FO <i>Denticulopsis praelauta</i>	16.3		16.2	No	2
FO <i>Crucidenticula kanayae</i>	16.9	16.7–17.1	16.7	Yes(Eq)	2
FO <i>Crucidenticula sawamurae</i>	18.4	18.3–18.5	17.55	Yes(Eq)	2
LO <i>Thalassiosira praefraga</i>	18.4		17.8	No(Eq)	2
FO <i>Thalassiosira fraga</i>	20.3?		20.1	Yes(So)	6

Notes: Source of ages for diatom events: 1 = Koizumi and Tanimura (1985), 2 = Barron (1992), 3 = Koizumi (1992), 4 = Gersonde and Burckle (1990), 5 = Harwood and Maruyama (1992), 6 = Baldauf and Barron (1991), and 7 = Bodén (1993). See Table 1 caption for further explanation. PM? = paleomagnetic calibration? Asterisk (\*) = correlated between Holes 887A and 887C by GRAPE events. So = Southern Ocean, and Eq = equatorial Pacific Ocean.

**Table 7.** Comparison of ages of latest Miocene through Pleistocene diatom datum levels derived from magnetostratigraphy in Leg 145 holes with published ages.

Datum	Site 884B	Site 887	Site 882	Site 883	Site 881	Published ages		
						Age (Ma)	PM?	Source
LO <i>Pyxidicula horridus</i>	1.8–2.0		1.6–1.8	1.6–1.8		1.8	No	2
LO <i>Pyxidicula pustulata</i>	2.0–2.2		1.9–2.1			1.8	No	8
LO <i>Neodenticula koizumii</i>	2.0–2.2		2.0–2.1	1.6–1.8		1.9–2.1	Yes	3
LO <i>Pyxidicula zabelinae</i>	2.0–2.2					2.8–3.13	Yes	3
LO <i>Thalassiosira marujamica</i>	3.1–3.2	3.25	3.1–3.2	3.1	3.1–3.2	3.05–3.45	Yes	3
LO <i>Thalassiosira jacksonii</i>	3.7–3.8		3.3–3.4	3.1–3.2	3.1	3.25–4.05	Yes	3
FO <i>Neodenticula koizumii</i>	3.7–3.8	3.70	3.4	3.45–3.55	3.75–3.95	3.51–3.85	Yes	1
FO <i>Actinocyclus oculus</i>	3.9	3.65	3.6–3.7	3.7	3.75–3.95	2.3–3.85	Yes	3
LO <i>Thalassiosira jacksonii</i> (plicate)	4.6	4.8 (d)	4.5–4.6	4.5–4.6				
LO <i>Thalassiosira insigna</i>	4.7–4.8			4.5–4.7		4.6	No	2
FO <i>Thalassiosira tertaria</i>	4.85							
FO <i>Thalassiosira latimarginata</i> s.str.	4.9	5.0	4.8–4.9	4.8–4.9		5.05–5.7	No	3
FO <i>Thalassiosira jacksonii</i> (plicate)	5.0	5.0	4.9–5.1					
FO <i>Thalassiosira latimarginata</i> s. ampl.	5.3		4.9–5.1					
FO <i>Thalassiosira oestrupii</i>	5.3	5.3*				5.4; 5.7	Yes	2; 1

Notes: See captions of Tables 1 and 6 for further explanation, with the addition of 8 = Barron (1980). (d) = dissolution controlled.

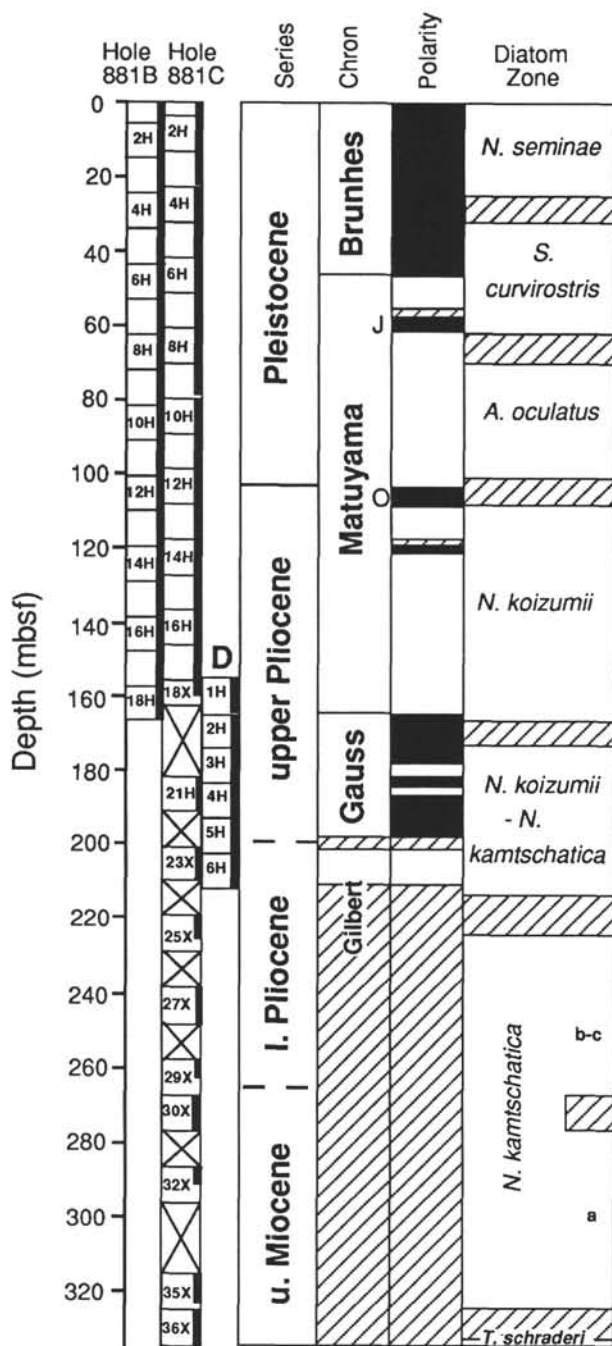


Figure 7. Stratigraphic position of cores, recovery (black), ages, placement of magnetostratigraphic chronos and subchrons, and placement of diatom zones in Holes 881B, 881C, and 881D. The magnetostratigraphy shown is that of Shipboard Scientific Party (1993a). Intervals filled by slanted lines indicate uncertainty in the placement of magnetostratigraphic and biostratigraphic boundaries and/or absence of paleomagnetic stratigraphy.

for the FO of *Actinocyclus oculatus* (3.9–3.6 Ma), the FO of *Neodenticula koizumii* (3.75–3.4 Ma), and the LO of *Neodenticula koizumii* (ca. 2.0–1.7 Ma).

#### ACKNOWLEDGMENTS

We thank Fumio Akiba, Lloyd Burckle, Itaru Koizumi, William V. Sliter, and Lisa D. White for their helpful reviews and suggestions for

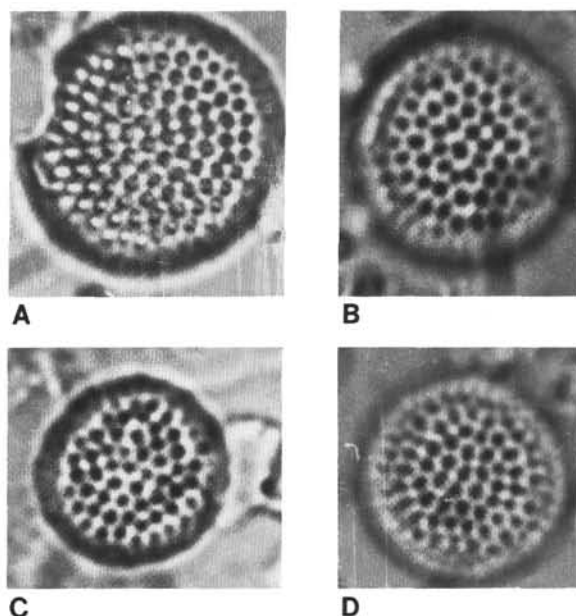


Figure 8. *Thalassiosira minutissima* Oreshkina, sp. nov. Magnification  $\times 3500$ .  
**A.** Isotype, Slide #4596/4, Sample 19-192-25R-2, 40–42 cm. **B.** Sample 86-581-6R-6, 101–102 cm, northwest Pacific. **C.** Isotype, Slide #44596/4, Sample 19-192-25R-2, 40–42 cm. **D.** Holotype, Slide #4596/4, Geological Institute, Russian Academy of Science (Moscow), Sample 19-192-25R-2, 40–42 cm, Meiji Seamount, northwest Pacific.

improving the manuscript. Scott Starratt also provided editorial comments. The research of Andrey Gladennov was supported by Grant #93-05-9558 of the Russian Foundation for Fundamental Research and in part by a JOI travel grant to Russian scientists. We are grateful to David Rea, Ivan Basov, and the scientists and crew members of Leg 145 of the JOIDES Resolution for their support and encouragement.

#### APPENDIX

##### New Species

We have invited Tatjana Oreshkina to formally publish this new species here, because she had described this form in her unpublished Ph.D. dissertation.

*Thalassiosira minutissima* Oreshkina, nov. sp.  
(Figs. 8A–D)

*Thalassiosira praeconvexa* Burckle sensu Schrader, 1973, pl. 11, figs. 10–15

*Thalassiosira* sp. 1 sensu Barron, 1980a, pl. 5, figs. 6, 7

*Thalassiosira* sp. 1 sensu Barron, 1981, pl. 5, fig. 5

*Thalassiosira* sp. 1 of Barron sensu Koizumi and Tanimura, 1985, pl. 4, figs.

1–3

*Thalassiosira praeconvexa* Schrader sensu Oreshkina, 1985, pl. 2, figs. 1, 2

*Thalassiosira* cf. *praeconvexa* Schrader sensu Akiba, 1986, pl. 8, fig. 5

*Thalassiosira* sp. 1 sensu Barron 1980 in Baldauf and Barron, pl. 1, figs. 3, 5, 6

**Description.** Valve circular, convex, slightly depressed in the center, 8–10  $\mu\text{m}$  in diameter. Areolae tangentially arranged, somewhat disordered, isolated from each other, 7–8 in 10  $\mu\text{m}$ . Areolae on the mantle finer, 12–15 in 10  $\mu\text{m}$ . On the valve face 1–2 mucous pores are present near the center. Margin striated with about 16 striae in 10  $\mu\text{m}$  and a ring of short spines, 10 in 10  $\mu\text{m}$ .

**Remarks.** *Thalassiosira minutissima* is a reliable stratigraphic marker in the upper part of the *Denticulopsis dimorpha* Zone and the *D. katayamiae* Zone in the North Pacific. It also occurs during the approximately same stratigraphic interval in the Southern Ocean (Baldauf and Barron, 1991; Harwood and Maruyama, 1992).

**Holotype.** Figure 8D, Sample 19-192-25R-2, 40–42 cm, Meiji Seamount, northwest Pacific. Slide #4596/4 deposited in the Geological Institute, Russian Academy of Science Collection (Moscow).

**Isotypes.** Figures 8A and 8C, Sample 19-192-25R-2, 40–42 cm. Slide #4596/4 deposited in the Geological Institute, Russian Academy of Science Collection (Moscow).

#### Taxonomic References

Stratigraphically important early middle Miocene and older taxa are treated and illustrated in Gladenkov and Barron (this volume). For stratigraphically important younger taxa, the taxon's formal citation is given along with important synonyms. In general, only a reference to representative illustrations (separated from the taxon's name by a semicolon) is provided, and the reader is referred to these references for a more thorough taxonomic treatment.

- Actinocyclus curvatus* Janisch; Koizumi, 1973, pl. 1, figs. 1–6
- Actinocyclus oculatus* Jousé; Barron, 1980a, pl. 5, figs. 1, 3
- Azpetia nodulifera* (Schmidt) Fryxell et Sims = *Coscinodiscus nodulifer* Schmidt; Akiba, 1986, pl. 2, figs. 6–7, pl. 3, fig. 6
- Crucicula nicobarica* (Grunow) Akiba et Yanagisawa; Akiba, 1986, pl. 26, figs. 1–4
- Denticulopsis crassa* Yanagisawa et Akiba, 1990, p. 248, pl. 3, figs. 21–27, pl. 12, figs. 1–8
- Denticulopsis dimorpha* (Schrader) Simonsen; Akiba, 1986, pl. 26, fig. 9; pl. 27, figs. 1–13
- Denticulopsis hustedtii* (Simonsen et Kanaya) Simonsen; Akiba, 1986, pl. 28, figs. 5–18
- Denticulopsis hyalina* (Schrader) Simonsen; Akiba, 1986, pl. 26, figs. 20–25
- Denticulopsis katayamae* Maruyama; Akiba, 1986, pl. 28, figs. 1–4
- Denticulopsis praedimorpha* Barron ex Akiba; Akiba, 1986, pl. 26, fig. 8; pl. 27, figs. 14–26
- Hemidiscus cuneiformis* Wallich; Akiba, 1986, pl. 16, figs. 3–4
- Neodenticula kamtschatica* (Zabelina) Akiba et Yanagisawa; Akiba, 1986, pl. 25, figs. 7–27
- Neodenticula koizumii* Akiba et Yanagisawa = *Denticulopsis seminae* f. *fossilis* Koizumi, 1973, pl. 5, figs. 30, 37, 38
- Neodenticula seminae* (Simonsen et Kanaya) Akiba et Yanagisawa in Akiba, 1986, pl. 25, figs. 28–32
- Nitzschia fossilis* (Frenguelli) ex Schrader; Akiba, 1986, pl. 22, figs. 1, 2, 3(?)
- Nitzschia grunowii* Hasle; Akiba, 1986, pl. 24, figs. 19–21
- Nitzschia heteropolica* Schrader; Akiba, 1986, pl. 23, fig. 3
- Nitzschia miocenica* Burckle; Akiba, 1986, pl. 23, figs. 10, 14
- Nitzschia ploicena* (Brun) Mertz; Akiba, 1986, pl. 23, figs. 6–9
- Nitzschia praereinholdii* Schrader, 1973, p. 708; pl. 5, figs. 20, 23–26
- Nitzschia reinholdii* Kanaya ex Schrader; Akiba, 1986, pl. 22, figs. 4–5
- Nitzschia rolandii* Schrader; Akiba, 1986, pl. 25, figs. 1–6
- Nitzschia suikoensis* Koizumi, 1980, pl. 1, figs. 1–6
- Porosira punctata* (Jousé) Makarova, 1988, p. 1184, pl. 1, figs. 1–16 = *Thalassiosira punctata* Jousé; Akiba, 1986, pl. 9, figs. 5, 6
- Pseudopodosira elegans* Sheshukova-Poretskaya; Akiba, 1986, pl. 4, figs. 5–7
- Pyxidicula horridus* (Koizumi) Oreshkina in Gladenkov et al., 1992, p. 201, pl. XLVI, figs. 8–10 = *Stephanopyxis horridus* Koizumi, 1972, p. 348, pl. 42, figs. 1a–2b; Koizumi, 1973, pl. 6, figs. 1–4
- Pyxidicula pustulata* (Mann) Oreshkina in Gladenkov et al., 1992, p. 201, pl. XLV, figs. 7–9 = *Coscinodiscus pustulatus* Mann, 1907, p. 257, pl. 48, fig. 3; Koizumi, 1973, pl. 4, figs. 1–4
- Pyxidicula zabelinae* (Jousé) Makarova et Moiseyeva, 1986, p. 244, pl. 1, figs. 2–25; pl. 2, figs. 1–15 = *Thalassiosira zabelinae* Jousé; Akiba, 1986, pl. 8, fig. 11
- Rhizosolenia matuyamai* Burckle; Barron, 1980b, pl. 7, figs. 9–12
- Rossiella tatsunokuchiensis* (Koizumi) Gersonde et Schrader; Akiba, 1986, pl. 19, figs. 7–12
- Rouxia californica* Peragallo; Akiba, 1986, pl. 21, figs. 5–6
- Simonsenella barbii* (Brun) Fenner, 1991, p. 108 = *Rhizosolenia barbii* (Brun) Tempère et Peragallo; Akiba, 1986, pl. 18, fig. 2
- Simonsenella curvirostris* (Jousé) Fenner, 1991, p. 108, pl. 3, figs. 1, 3 = *Rhizosolenia curvirostris* Jousé; Akiba, 1986, pl. 18, fig. 3
- Thalassionema robusta* Schrader, 1973, p. 712, pl. 23, figs. 24, 35–37
- Thalassionema schraderi* Akiba; Akiba, 1986, pl. 21, figs. 13–16
- Thalassiosira convexa* Muchina; Akiba, 1986, pl. 8, fig. 1
- Thalassiosira gravida* Cleve; Akiba, 1986, pl. 10, figs. 1–4
- Thalassiosira insignia* (Jousé) Harwood et Maruyama = *Cosmiodiscus insignis* Jousé; Akiba, 1986, pl. 17, fig. 1
- Thalassiosira jacksonii* Koizumi et Barron; Akiba, 1986, pl. 11, fig. 2
- Thalassiosira jacksonii* (plicate form).

**Remarks.** Plicate specimens of *T. jacksonii* are included here.

- Thalassiosira jouseae* Akiba, 1985, pl. 6, figs. 8–10 = *Thalassiosira nidulus* (Tempère et Brun) Jousé sensu Barron, 1980a, pl. 6, fig. 5
- Thalassiosira latimarginata* Makarova, 1975, p. 150, figs. 3, 4 = *T. trifulta* Fryxell, Akiba, 1986, pl. 10, figs. 5, 7 (not 6); = *Coscinodiscus excentricus* Ehr., sensu Koizumi, 1973, pl. 2, figs. 11–12; = *C. excentricus* var. *fasciculata* Hust. sensu Koizumi, 1973, pl. 2, figs. 13–16; = *C. excentricus* var. *jousei* Kanaya sensu Koizumi, 1973, pl. 3, figs. 1–6; = *C. excentricus* var. *leasareolatus* Kanaya sensu Koizumi, 1973, pl. 3, figs. 7–11
- Thalassiosira latimarginata* Makarova s. ampl.

**Remarks.** Forms closely resembling *T. latimarginata* but lacking a definite trilobite arrangement of central processes (such as in *T. trifulta* Fryxell, Akiba, 1986, pl. 10, fig. 6) are included here.

- Thalassiosira manifesta* Sheshukova-Poretskaya; Akiba, 1986, pl. 9, figs. 1–3

*Thalassiosira marujamica* Sheshukova-Poretskaya; Akiba, 1986, pl. 13, figs. 1–7; = *Thalassiosira nativa* Sheshukova-Poretskaya sensu Barron, 1980a, pl. 6, figs. 8–9?

- Thalassiosira miocenica* Schrader; Barron, 1985b, pl. 11, fig. 11

*Thalassiosira oestrupii* (Ostenfeld) Proshkina-Lavrenko; Akiba, 1986, pl. 14, figs. 1–6

**Remarks.** The Pliocene forms are probably *T. tetraoestrupii* Bodén, 1993, p. 63, pl. 1, figs. A–G, and pl. 2, figs. A, B, H, and J. However, these two forms are difficult to distinguish from each other in the light microscope, so no effort was made to tabulate them separately.

- Thalassiosira praeoestrupii* Dumont, Baldauf, et Barron; Bodén, 1993, p. 67, pl. 1, figs. H–J; pl. 2, figs. C–F, I

*Thalassiosira singularis* Sheshukova-Poretskaya; Akiba, 1986, pl. 12, figs. 6–8

- Thalassiosira tertaria* Sheshukova-Poretskaya, 1967, pl. 15, fig. 2

#### REFERENCES\*

- Akiba, F., 1986. Middle Miocene to Quaternary diatom biostratigraphy in the Nankai trough and Japan trench, and modified lower Miocene through Quaternary diatom zones for middle-to-high latitudes of the North Pacific. In Kagami, H., Karig, D.E., Coulbourn, W.T., et al., *Init. Repts. DSDP*, 87: Washington (U.S. Govt. Printing Office), 393–481.
- Akiba, F., Hiramatsu, C., and Yanagisawa, Y., 1993. A Cenozoic diatom genus *Cavittatus* Williams: an emended description and two new biostratigraphically useful species, *C. lanceolatus* and *C. rectus* from Japan. *Bull. Nat. Sci. Mus. Ser. C.: Geol. Paleontol. (Tokyo)*, 19:11–39.
- Akiba, F., and Yanagisawa, Y., 1986. Taxonomy, morphology and phylogeny of the Neogene diatom zonal marker species in the middle-to-high latitudes of the North Pacific. In Kagami, H., Karig, D.E., Coulbourn, W.T., et al., *Init. Repts. DSDP*, 87: Washington (U.S. Govt. Printing Office), 483–554.
- Baldauf, J.G., and Barron, J.A., 1991. Diatom biostratigraphy: Kerguelan Plateau and Prydz Bay regions of the Southern Ocean. In Barron, J., Larsen, B., et al., *Proc. ODP, Sci. Results*, 119: College Station, TX (Ocean Drilling Program), 547–598.
- Baldauf, J.G., Thomas, E., Clement, B., Takayama, T., Weaver, P.P.E., Backman, J., Jenkins, G., Mudie, P.J., and Westberg-Smith, M.J., 1987. Magnetostratigraphic and biostratigraphic synthesis, Deep Sea Drilling Project Leg 94. In Ruddiman, W.F., Kidd, R.B., Thomas, E., et al., *Init. Repts. DSDP*, 94 (Pt. 2): Washington (U.S. Govt. Printing Office), 1159–1205.
- Barron, J.A., 1980a. Lower Miocene to Quaternary diatom biostratigraphy of Leg 57, off Northeastern Japan, Deep Sea Drilling Project. In von Huene, R., Nasu, N., et al., *Init. Repts. DSDP*, 56, 57 (Pt. 2): Washington (U.S. Govt. Printing Office), 641–686.
- , 1980b. Upper Pliocene and Quaternary diatom biostratigraphy of Deep Sea Drilling Project Leg 54, tropical eastern Pacific. In Rosendahl, B.R., Hekinian, R., et al., *Init. Repts. DSDP*, 54: Washington (U.S. Govt. Printing Office), 455–485.
- , 1981. Late Cenozoic diatom biostratigraphy and paleoceanography of the middle-latitude eastern North Pacific, Deep Sea Drilling Project Leg 63. In Yeats, R.S., Haq, B.U., et al., *Init. Repts. DSDP*, 63: Washington (U.S. Govt. Printing Office), 507–538.
- , 1985a. Late Eocene to Holocene diatom biostratigraphy of the equatorial Pacific Ocean, Deep Sea Drilling Project Leg 85. In Mayer, L.,

\* Abbreviations for names of organizations and publications in ODP reference lists follow the style given in *Chemical Abstracts Service Source Index* (published by American Chemical Society).

- Theyer, F., Thomas, E., et al., *Init. Repts. DSDP*, 85: Washington (U.S. Govt. Printing Office), 413–456.]
- \_\_\_\_\_, 1985b. Miocene to Holocene planktic diatoms. In Bolli, H.M., Saunders, J.B., and Perch-Nielsen, K. (Eds.), *Plankton Stratigraphy*: Cambridge (Cambridge Univ. Press), 763–809.
- \_\_\_\_\_, 1989. The late Cenozoic stratigraphic record and hiatuses of the Northeast Pacific: results from the Deep Sea Drilling Project. In Winterer, E.L., Hussong, D.M., and Decker, R.W. (Eds.), *The Geology of North America* (Vol. N): *The Eastern Pacific Ocean and Hawaii*. Geol. Soc. Am., Geol. of North America Ser., 311–322.
- \_\_\_\_\_, 1992. Neogene diatom datum levels in the equatorial and North Pacific. In Ishizaki, K., and Saito, T. (Eds.), *The Centenary of Japanese Micropaleontology*: Tokyo (Tokyo Univ. Press), 413–425.
- Basilian, A.E., Barinov, K.B., Oreshkina, T.V., and Trubikhin, V.N., 1991. Bering Sea transgressions in Pliocene. In *Pliocene Anthropogene Paleogeography and Biostratigraphy*. Proc. 13th INQUA Congr., Moscow, 5–24. (in Russian)
- Berggren, W.A., Kent, D.V., and Flynn, J.J., 1985a. Jurassic to Paleogene: Part 2. Paleogene geochronology and chronostratigraphy. In Snelling, N.J. (Ed.), *The Chronology of the Geological Record*. Geol. Soc. London Mem., 10:141–195.
- Berggren, W.A., Kent, D.V., and Van Couvering, J.A., 1985b. The Neogene: Part 2. Neogene geochronology and chronostratigraphy. In Snelling, N.J. (Ed.), *The Chronology of the Geological Record*. Geol. Soc. London Mem., 10:211–260.
- Bodén, P., 1993. Taxonomy and stratigraphic occurrence of *Thalassiosira tetraoestrupii* sp. nov. and related species in upper Miocene and lower Pliocene sediments from the Norwegian Sea, North Atlantic and northwest Pacific. *Terra Nova*, 5:61–75.
- Burckle, L.H., and Opdyke, N.D., 1977. Late Neogene diatom correlations in the Circum-Pacific. In Ujié, H., and Saito, T. (Eds.), *Proc. 1st Int. Congr. Pac. Neogene Stratigr.* Tokyo (Kaiyo Shupan), 255–284.
- Cande, S.C., and Kent, D.V., 1992. A new geomagnetic polarity time scale for the Late Cretaceous and Cenozoic. *J. Geophys. Res.*, 97:13917–13951.
- Fenner, J.M., 1991. Late Pliocene-Quaternary quantitative diatom stratigraphy in the Atlantic sector of the Southern Ocean. In Ciesielski, P.F., Kristoffersen, Y., et al., *Proc. ODP, Sci. Results*, 114: College Station, TX (Ocean Drilling Program), 97–121.
- Gersonde, R., and Burckle, L.H., 1990. Neogene diatom biostratigraphy of ODP Leg 113, Weddell Sea (Antarctic Ocean). In Barker, P.F., Kennett, J.P., et al., *Proc. ODP, Sci. Results*, 113: College Station, TX (Ocean Drilling Program), 761–789.
- Gladenkov, Y.B., Barinov, K.B., Basilian, A.E., Bordunov, S.I., Bratseva, G.M., Zyryanov, Y.V., Kuralenko, N.P., Vitukhin, D.I., Oreshkina, T.V., Ganzei, S.S., Kiyashko, S.I., and Trubikhin, 1992. *Detailed Division of the Neogene of Kamchatka*. Russian Acad. Sci., Trans, 478: Moscow (Nauka).
- Harwood, D.M., and Maruyama, T., 1992. Middle Eocene to Pleistocene diatom biostratigraphy of Southern Ocean sediments from the Kerguelen Plateau, Leg 120. In Wise, S.W., Jr., Schlich, R., et al., *Proc. ODP, Sci. Results*, 120: College Station, TX (Ocean Drilling Program), 683–733.
- Koizumi, I., 1972. Marine diatom flora of the Pliocene Tatsunokuchi Formation in Fukushima Prefecture. *Trans. Proc. Paleontol. Soc. Jpn.*, New Ser., 86:340–359.
- \_\_\_\_\_, 1973. The late Cenozoic diatoms of Sites 183–193, Leg 19 Deep Sea Drilling Project. In Creager, J.S., Scholl, D.W., et al., *Init. Repts. DSDP*, 19: Washington (U.S. Govt. Printing Office), 805–855.
- \_\_\_\_\_, 1975. Neogene diatoms from the northwestern Pacific Ocean, Deep Sea Drilling Project. In Larson, R.L., Moberly, R., et al., *Init. Repts. DSDP*, 32: Washington (U.S. Govt. Printing Office), 865–889.
- \_\_\_\_\_, 1980. Neogene diatoms from the Emperor Seamount Chain, Leg 55, Deep Sea Drilling Project. In Jackson, E.D., Koizumi, I., et al., *Init. Repts. DSDP*, 55: Washington, (U.S. Govt. Printing Office), 387–400.
- \_\_\_\_\_, 1985. Diatom biochronology for the Late Cenozoic northwest Pacific. *Chishitsugaku Zasshi [J. Geol. Soc. Japan]*, 91:195–211.
- \_\_\_\_\_, 1992. Diatom biostratigraphy of the Japan Sea: Leg 127. In Piscesotto, K., Ingle, J.C., Jr., von Breymann, M., and Barron, J.A., et al., *Proc. ODP, Sci. Results*, 127/128 (Pt. 1): College Station, TX (Ocean Drilling Program), 249–289.
- Koizumi, I., and Tanimura, Y., 1985. Neogene diatom biostratigraphy of the middle latitude western North Pacific, Deep Sea Drilling Project Leg 86. In Heath, G.R., Burckle, L.H., et al., *Init. Repts. DSDP*, 86: Washington (U.S. Govt. Printing Office), 269–300.
- Makarova, I.V., 1975. New species of the genus *Thalassiosira* Cleve from the Barents Sea. *Nov. Syst. Nizshih Rast.*, 12:149–152. (in Russian)
- \_\_\_\_\_, 1988. New combinations of taxa from the late Miocene and early Pliocene diatom floras of Sakhalin. *Bot. Zh.* (Leningrad), 73:1183–1186. (in Russian)
- Makarova, I.V., and Moiseyeva, A.I., 1986. A new species of the genus *Pyxidicula* (Bacillariophyta). *Bot. Zh.* (Leningrad), 71:244–245. (in Russian)
- Mann, A., 1907. Report on the diatoms of the *Albatross* voyage in the Pacific Ocean, 1888–1904. *Contrib. U.S. Nat. Herb.*, 10:221–419.
- Maruyama, T., 1984. Miocene diatom biostratigraphy of onshore sequences on the Pacific side of Northeast Japan, with reference to DSDP Hole 438A (Part 2). *Sci. Rep. Tohoku Univ.*, Ser. 2, 55:77–140.
- Berggren, W.A., Kent, D.V., and Van Couvering, J.A., 1985b. The Neogene: Part 2. Neogene geochronology and chronostratigraphy. In Snelling, N.J. (Ed.), *The Chronology of the Geological Record*. Geol. Soc. London Mem., 10:211–260.
- Oreškina, T.V., 1985. Diatom associations and the stratigraphy of the upper Cenozoic of the Pacific region near Kamchatka. *Izv. Akad. Nauk SSSR, Ser. Geol.*, 5:60–73. (in Russian)
- Rea, D.K., Basov, I.A., Janecek, T.R., Palmer-Julson, A., et al., 1993. *Proc. ODP, Init. Repts.*, 145: College Station, TX (Ocean Drilling Program).
- Sancetta, C., and Silvestri, S., 1986. Pliocene-Pleistocene evolution of the North Pacific ocean-atmosphere system, interpreted from fossil diatoms. *Paleoceanography*, 1:163–180.
- Schrader, H.-J., 1973. Cenozoic diatoms from the Northeast Pacific, Leg 18. In Kulm, L.D., von Huene, R., et al., *Init. Repts. DSDP*, 18: Washington (U.S. Govt. Printing Office), 673–797.
- Sheshukova-Poretskaya, V.S., 1967. *Neogene Marine Diatoms of Sakhalin and Kamchatka*: Leningrad (Leningrad Univ.).
- Shipboard Scientific Party, 1993a. Site 881. In Rea, D.K., Basov, I.A., Janecek, T.R., Palmer-Julson, A., et al., *Proc. ODP, Init. Repts.*, 145: College Station, TX (Ocean Drilling Program), 37–83.
- \_\_\_\_\_, 1993b. Site 882. In Rea, D.K., Basov, I.A., Janecek, T.R., Palmer-Julson, A., et al., *Proc. ODP, Init. Repts.*, 145: College Station, TX (Ocean Drilling Program), 85–119.
- \_\_\_\_\_, 1993c. Site 883. In Rea, D.K., Basov, I.A., Janecek, T.R., Palmer-Julson, A., et al., *Proc. ODP, Init. Repts.*, 145: College Station, TX (Ocean Drilling Program), 121–208.
- \_\_\_\_\_, 1993d. Site 884. In Rea, D.K., Basov, I.A., Janecek, T.R., Palmer-Julson, A., et al., *Proc. ODP, Init. Repts.*, 145: College Station, TX (Ocean Drilling Program), 209–302.
- \_\_\_\_\_, 1993e. Site 887. In Rea, D.K., Basov, I.A., Janecek, T.R., Palmer-Julson, A., et al., *Proc. ODP, Init. Repts.*, 145: College Station, TX (Ocean Drilling Program), 335–391.
- Yanagisawa, Y., and Akiba, F., 1990. Taxonomy and phylogeny of three marine diatom genera, *Crucidenticula*, *Denticulopsis*, and *Neodenticula*. *Bull. Geol. Surv. Jpn. [Chishitsu Chosasho Geppo]*, 41:197–301.
- Zijderveld, J.D.A., Zachariasse, J.W., Verhallen, P.J.J.M., and Hilgen, F.J., 1986. The age of the Miocene-Pliocene boundary. *Newsl. Stratigr.*, 16:169–181.

Date of initial receipt: 5 April 1994

Date of acceptance: 15 July 1994

Ms 145SR-101